Molecular Pharmacology Fast Forward. Published on September 5, 2020 as DOI: 10.1124/molpharm.120.000103
This article has not been copyedited and formatted. The final version may differ from this version.

Title:

Antiepileptic drug-activated constitutive androstane receptor inhibits peroxisome proliferator-activated receptor α- and peroxisome proliferator-activated receptor γ coactivator 1α-dependent gene expression to increase blood triglyceride levels

Authors:

Ryota Shizu[1], Yuta Otsuka[2], Kanako Ezaki[1], Chizuru Ishii[2], Shingo Arakawa[3], Yuto Amaike[1], Taiki Abe[1,2], Takuomi Hosaka[1], Takamitsu Sasaki[1], Yuichiro Kanno[1], Masaaki Miyata[2], Yasushi Yamazoe[2], Kouichi Yoshinari[1,2]

Affiliations:

[1]Laboratory of Molecular Toxicology, School of Pharmaceutical Sciences, University of Shizuoka, 52-1 Yada, Suruga-ku, Shizuoka 422-8526 Japan. (RS, KE, YA, TA, TH, TS, YK, KY)

[2]Graduate School of Pharmaceutical Sciences, Tohoku University, 6-3 Aramaki-aoba, Aoba-ku, Sendai, Miyagi 980-8578, Japan. (YO, CI, TA, MM, YY, KY)

[3]Pharmacovigilance Department, Clinical Safety & Pharmacovigilance Division, Daiichi Sankyo Co., Ltd., 3-5-1, Nihonbashi-honcho, Chuo-ku, Tokyo 103-8426 Japan. (SA)

Molecular Pharmacology Fast Forward. Published on September 5, 2020 as DOI: 10.1124/molpharm.120.000103
This article has not been copyedited and formatted. The final version may differ from this version.

Running TITLE: CAR inhibits PPARα/PGC1α functions for triglyceride control

Corresponding author:

Kouichi Yoshinari, Ph.D.

Laboratory of Molecular Toxicology, School of Pharmaceutical Sciences, University of Shizuoka, 52-1 Yada, Suruga-ku, Shizuoka 422-8526 Japan

Email: yoshinari@u-shizoka-ken.ac.jp;

Telephone/fax.: +81-54-264-5685

The number of text pages: 28

The number of tables: 1

The number of figures: 10

The number of references: 51

Abstract: 196 words

Introduction: 584 words

Discussion: 1128 words

Abbreviations: AED, antiepileptic drug; AF2, activation function 2; CAR, constitutive active/androstane receptor; CITCO, 6-(4-chlorophenyl)imidazo[2,1-b][1,3]thiazole-5-carbaldehyde O-(3,4-dichlorobenzyl)oxime; DBD, DNA binding domain; DMEM, Dulbecco's Modified Eagle Medium; DMSO, dimethyl sulfoxide; EMSA, electrophoresis mobility shift assays; GRIP1, glucocorticoid receptor interacting protein1; HNF4α, hepatocyte nuclear factor 4α; LBD, ligand binding domain; PGC1α, peroxisome proliferator-activated receptor gamma coactivator-1α; PPAR, peroxisome proliferator-activated receptor; PPRE, peroxisome proliferator response element; PXR, pregnane X receptor; RXR, retinoid X receptor; TCPOBOP, 1,4-bis[2-(3,5-dichloropyridyloxy)]benzene; TG, triglyceride.

Molecular Pharmacology Fast Forward. Published on September 5, 2020 as DOI: 10.1124/molpharm.120.000103
This article has not been copyedited and formatted. The final version may differ from this version.

Abstract:

Long-term administration of some antiepileptic drugs often increases blood lipid levels. In this study, we investigated its molecular mechanism by focusing on the nuclear receptors constitutive active/androstane receptor (CAR) and peroxisome proliferator-activated receptor α (PPARα), which are key transcription factors for enzyme induction and lipid metabolism, respectively, in the liver. Treatment of mice with the CAR activator phenobarbital, an antiepileptic drug, increased plasma triglyceride levels and decreased the hepatic expression of PPARα target genes related to lipid metabolism. The increase in PPARα target gene expression induced by fenofibrate, a PPARα ligand, was inhibited by cotreatment with phenobarbital. CAR suppressed PPARα-dependent gene transcription in HepG2 cells but not in COS-1 cells. The mRNA level of peroxisome proliferator-activated receptor gamma coactivator-1α (PGC1α), a coactivator for both CAR and PPARα, in COS-1 cells was much lower than in HepG2 cells. In reporter assays with COS-1 cells overexpressing PGC1α, CAR suppressed PPARα-dependent gene transcription, depending on the coactivator-binding motif. In mammalian two-hybrid assays, CAR attenuated the interaction between PGC1α and PPARα. Chemical inhibition of PGC1α prevented phenobarbital-dependent increases in plasma triglyceride levels and the inhibition of PPARα target gene expression. These results suggest that CAR inhibits the interaction between PPARα and PGC1α, attenuating PPARα-dependent lipid metabolism. This might explain the antiepileptic drug-induced elevation of blood triglyceride levels.

Significance Statement:

CAR activated by antiepileptic drugs inhibits the PPARα-dependent transcription of genes related to lipid metabolism and upregulates blood TG levels. The molecular mechanism of this inhibition involves competition between these nuclear receptors for coactivator PGC1α binding.

Molecular Pharmacology Fast Forward. Published on September 5, 2020 as DOI: 10.1124/molpharm.120.000103
This article has not been copyedited and formatted. The final version may differ from this version.

Introduction:

Antiepileptic drugs (AEDs) are used worldwide by millions of people for the treatment of epilepsy. For most patients, long-term treatment with AEDs is required for the control of epileptic seizures. However, this long-term treatment occasionally causes side effects. Elevation of blood lipid levels is one of the well-known side effects of long-term AED treatment (Berlit et al., 1982; Verrotti et al., 1998; Zeitlhofer et al., 1993). Specifically, long-term AED therapy in epilepsy patients increased blood triglyceride levels and thus the risk of atherosclerosis (Chuang et al., 2012; Tan et al., 2009) and microangiopathy (Chen et al., 2018). AEDs consist of two groups: those inducing hepatic drug-metabolizing enzymes, such as phenobarbital, phenytoin and carbamazepine (enzyme-inducing AEDs), and those that do not induce drug-metabolizing enzymes, such as valproic acid, levetiracetam and lamotrigine. Generally, the former group increases blood lipid levels (Isojarvi et al., 1993; Livingston, 1976; Svalheim et al., 2010). Switching to AEDs that do not induce enzymes from enzyme-inducing AEDs can result in a significant reduction in total cholesterol and triglycerides (TGs) in the blood, as indicated in a clinical study (Mintzer et al., 2009).

Constitutive androstane/active receptor (CAR, NR1I3) is a xenobiotic-responsive nuclear receptor that is highly expressed in the liver and activated by numerous chemical compounds, including enzyme-inducing AEDs phenobarbital and carbamazepine (Sueyoshi et al., 1999; Timsit and Negishi, 2007; Wei et al., 2000). Upon chemical exposure, CAR, which is constitutively retained in the cytoplasm, accumulates in the nucleus and transactivates its target genes, including those encoding drug-metabolizing enzymes, e.g., cytochrome P450 isoforms, and drug transporters (Timsit and Negishi, 2007). To induce gene transcription, CAR heterodimerizes with retinoid X receptor α (RXRα, NR2B1) and binds to the promoter regions of target genes (Timsit and Negishi, 2007). The CAR/RXRα heterodimer recruits several coactivators, including glucocorticoid receptor-interacting protein 1 (GRIP1, NCOA2) and peroxisome proliferator-activated receptor gamma coactivator 1α (PGC1α), to their respective promoter regions, thereby accelerating the transcription of target genes (Min et al., 2002a; Shiraki et al., 2003).

Recent studies have revealed that CAR is also involved in hepatic energy metabolism, such as glucose and lipid metabolism. For example, treatment of obese mice models with the mouse CAR activator 1,4-

Molecular Pharmacology Fast Forward. Published on September 5, 2020 as DOI: 10.1124/molpharm.120.000103
This article has not been copyedited and formatted. The final version may differ from this version.

bis[2-(3,5-dichloropyridyloxy)]benzene (TCPOBOP) decreased blood glucose levels and ameliorated insulin resistance (Dong et al., 2009; Gao et al., 2009). In addition, CAR activation attenuated fatty acid metabolism by inhibiting the expression of genes related to fatty acid β-oxidation (Wada et al., 2009). The treatment of mice with a CAR activator decreased hepatic TG levels through the activation of Insig-1 along with reduced protein levels of the active form of sterol regulatory element-binding protein 1 or SREBP-1 (Roth et al., 2008). Taken with the fact that CAR is involved in the hepatic induction of drug-metabolizing enzymes, these results imply an association of CAR with the elevation of blood lipid levels by enzyme-inducing AEDs.

Nuclear receptor peroxisome proliferator-activated receptor α (PPARα, NR1C1) is highly expressed in the liver and plays critical roles in the regulation of lipid metabolism. Upon exposure to ligands, PPARα forms a heterodimer with RXRα to induce the transcription of target genes by recruiting coactivators. Fibrates, such as fenofibrate and bezafibrate, are typical PPARα ligand drugs and are used to lower blood TG levels *via* the expression of PPARα target genes (Berger and Moller, 2002).

In this study, to understand the molecular mechanism of the elevation of blood TG levels by CAR-activating enzyme-inducing AEDs, we have raised a hypothesis that CAR interferes with PPARα by competing with the coactivator PGC1α for blood TG level regulation and tested this hypothesis.

Materials and Methods:

Reagents

Phenobarbital and TCPOBOP were purchased from Sigma-Aldrich (St Louis, MO). 6-(4-Chlorophenyl)imidazo[2,1-*b*][1,3]thiazole-5-carbaldehyde *O*-(3,4-dichlorobenzyl)oxime (CITCO) was obtained from Merck (Darmstadt, Germany). Bezafibrate and fenofibrate were purchased from Fujifilm Wako Pure Chemical Industries (Osaka, Japan). SR18292 was obtained from Cayman Chemical (Ann Arbor, MI). Antibody against PGC1α, Anti-PGC-1, C-terminal (777-797) was purchased from Calbiochem (San Diego, CA). Anti-His-tag (PM002) and Anti-V5 tag (M167-3) were purchased from Medical and Biological Laboratories (Nagoya, Japan). Anti-human PPARα antibody (PP-H0723-00) was

Molecular Pharmacology Fast Forward. Published on September 5, 2020 as DOI: 10.1124/molpharm.120.000103
This article has not been copyedited and formatted. The final version may differ from this version.

from Perseus proteomics (Tokyo, Japan). siRNA targeting PGC1α and control siRNA, ON-TARGET *plus* Human PGC1α siRNA SMARTpool and ON-TARGET *plus* Non-targeting Control Pool were purchased from Dharmacon (Boulder, CO). Oligonucleotides were commercially synthesized by Fasmac (Atsugi, Japan). Restriction enzymes were purchased from New England Biolabs (Ipswich, MA). All other reagents were obtained from Fujifilm Wako Pure Chemical Industries or Sigma-Aldrich, unless otherwise indicated.

Plasmid Preparation

DNA fragments of mouse (m) *Hmgcs2* and human (h) *HMGCS2* were amplified with KOD Plus Neo (TOYOBO, Osaka, Japan) and cloned into pGL4.10 vectors (Promega, Madison, WI). $(NR1)_5$-tk-pGL3 plasmid was previously described (Benoki et al., 2012; Sueyoshi et al., 1999). The phRL-TK, phRL-CMV, phRL-SV40 and pGL4.31 plasmids were obtained from Promega. hCAR, mCAR, hPPARα and mPPARα cDNA were amplified by PCR and cloned into pTargeT vectors (Promega) to obtain the corresponding expression plasmids. hCAR, hPPARα and hRXRα cDNA were cloned into pTNT vectors (Promega). The sequence of the V5 epitope tag was inserted into the C-terminal of hCAR for DNA-affinity assay. A series of pFN21A plasmids expressing a coactivator, SRC1 (NCOA1), GRIP1, ACTR (NCOA3), ASC2 (NCOA6), PGC1α or NRIP1 were purchased from Promega. PBP (MED1) cDNA was amplified and inserted into the pFN21A plasmid (Promega). The double-stranded oligo-DNA encoding the nuclear receptor-binding motif (LXXLL motif) of PGC1α (5'-GAGGCAGAAGAGCCGTCTCTACTTAAGAAGCTCTTACTGGCACCAGCCAACACTCAGTGA-3') was inserted into the pFN11A plasmid (Promega). Intact hCAR and hPPARα cDNA were inserted into the pFN10A plasmid (Promega). All mutation or deletion constructs were prepared using a KOD Plus mutagenesis kit (TOYOBO) with specific primer sets.

Animal Experiments

Male C57BL/6N mice (approximately 7 weeks old obtained from Charles River Laboratories Japan,

Molecular Pharmacology Fast Forward. Published on September 5, 2020 as DOI: 10.1124/molpharm.120.000103
This article has not been copyedited and formatted. The final version may differ from this version.

Yokohama, Japan) were maintained under a 12-h light/12-h dark cycle and fed a conventional CE-2 laboratory diet (CLEA Japan, Tokyo, Japan) and given access to water ad libitum for one week to acclimatize them. The mice were injected intraperitoneally with TCPOBOP (3 mg/kg, dissolved in corn oil) or vehicle once daily for 5 consecutive days, and their livers were collected for DNA microarray analysis. For experiments to study fenofibrate and TCPOBOP cotreatment, the mice were fed a normal CE-2 diet supplemented with or without fenofibrate (300 ppm) for 2 weeks. Then, TCPOBOP (3 mg/kg, dissolved in corn oil) or vehicle was intraperitoneally injected for 5 consecutive days. Twenty-four hours after the last injection, the mouse livers were collected and subjected to qRT-PCR. For experiments based on fenofibrate and phenobarbital cotreatment, the mice were fed a normal CE-2 diet supplemented with phenobarbital (300 or 1000 ppm) and/or fenofibrate (300 or 1000 ppm) for 1 week, and their plasma and livers were collected. For studies with SR18292, the mice were intraperitoneally injected with phenobarbital (100 mg/kg, in saline) in combination with or without SR18292 (45 mg/kg, in corn oil) for 24 h. Then, their plasma and livers were collected.

Plasma TG concentration under the fed condition was determined using the Triglyceride E Test WAKO kit (Fujifilm Wako Pure Chemicals) following the manufacturer's instructions.

All animal experiments were approved by the committees for animal experiments at Tohoku University and University of Shizuoka and conducted in accordance with the guidelines for animal experiments at Tohoku University and University of Shizuoka.

DNA Microarray Analysis

Total RNA was prepared from the mouse livers. A DNA microarray analysis was performed using GeneSQUARE multiple assay DNA microarray metabolic syndromes for mice by Kurabo Industries (Kurashiki, Japan) with 3 mice per group.

Cell Culture

HepG2 and COS-1 cells (RIKEN BioResourse Center, Tsukuba, Japan) were cultured in Dulbecco's

Molecular Pharmacology Fast Forward. Published on September 5, 2020 as DOI: 10.1124/molpharm.120.000103
This article has not been copyedited and formatted. The final version may differ from this version.

modified Eagle's medium (DMEM) (Fujifilm Wako Pure Chemicals) supplemented with heat-inactivated 10% fetal bovine serum (BIOWEST, Nuaillé, France), nonessential amino acids (Gibco) and antibiotic-antimycotic (Gibco). The cells were seeded in 96-well plates (BD Biosciences, Heidelberg, Germany) at 1 × 10^4 cells/well. Twenty-four hours after the seeding, plasmid transfection was conducted.

Cryopreserved human hepatocytes (Lot. HEP187111: White, female, 56 years old) were purchased from Biopredic International (Rennes, France). Cells were thawed and plated onto collagen-coated 48-well plates (BD Biosciences) at a density of 1 × 10^5 cells/well and maintained in KHEM5310 medium (KAC, Kyoto, Japan) supplemented with 10% fetal bovine serum (BIOWEST) for 4 h at 37°C. The medium was then changed to serum-free Williams' E medium (Thermo Fisher Scientific, Waltham, MA) containing 0.1 μM dexamethasone (Sigma-Aldrich), ITS-PREMIX (BD Biosciences), 100 U/ml penicillin, 100 μg/ml streptomycin. After 24 h of culture, the cells were treated with drugs for 48 h and harvested for RNA extraction. Total RNA was subjected to qRT-PCR.

HepaRG cells (Thermo Fisher Scientific) were seeded in collagen type I–coated 48-well plates at a density of 2 × 10^5 cells/well and maintained in William's E medium supplemented with GlutaMAX supplement (Thermo Fisher Scientific) and HepaRG Thaw, Plate, & General Purpose Medium Supplement (Thermo Fisher Scientific) for 6 h. Then, the medium was changed to fresh medium. After 72 h of culture, the cells were treated with drugs diluted in William's E medium supplemented with GlutaMAX supplement and HepaRG Serum-free Induction Medium Supplement (Thermo Fisher Scientific) for 48 h and harvested for RNA extraction. Total RNA was subjected to quantitative reverse transcription-PCR (qRT-PCR).

qRT-PCR

Total RNA was isolated using Sepasol RNA I (Nacalai Tesque, Kyoto, Japan). The measurement of mRNA levels was performed as described previously (Abe et al., 2018). The sequences of the primers used for qRT-PCR are shown in Table S2.

Molecular Pharmacology Fast Forward. Published on September 5, 2020 as DOI: 10.1124/molpharm.120.000103
This article has not been copyedited and formatted. The final version may differ from this version.

Reporter Assay

Twenty-four hours after the seeding, the cells were cotransfected with the reporter, expression and *Renilla* luciferase-expressing plasmids using Lipofectamine 3000 (Invitrogen, Carlsbad, CA) and treated with vehicle (0.1% or 0.2% DMSO) or drugs in serum-free DMEM for 24 h. siRNA targeting PGC1α or control siRNA was transfected with Lipofectamine RNAiMAX (Invitrogen) 48 h before reporter plasmid transfection. Reporter activity was measured using Dual-Luciferase Reporter Assay System (Promega) following the manufacturer's instructions. Firefly luciferase luminescence was normalized to *Renilla* luciferase luminescence.

Mammalian Two-hybrid Assay

HepG2 cells were seeded in 96-well plates (BD Biosciences) at 1×10^4 cells/well. Twenty-four hours later, the cells were transfected with pGL4.31, the pFN11A-based expression plasmid for the PGC1α-LXXLL motif (EAEEPSLLKKLLLAPANTQ) fused with the GAL4 DNA binding domain (DBD) protein, the pFN10A-based expression plasmid for CAR or PPARα fused with the VP-16 transactivation domain, and the *Renilla* luciferase expressing plasmid phRL-CMV using Lipofectamine 3000. The cells were then treated with vehicle (0.1% or 0.2% DMSO) or drugs in serum-free DMEM for 24 h, and the reporter activity was measured with Dual-Luciferase Reporter Assay System.

Electrophoresis Mobility Shift Assay (EMSA)

EMSAs were performed as described previously (Yoshinari et al., 2010). Briefly, hCAR, hPPARα and hRXRα were synthesized with a pTNT plasmid using a TnT SP6 Quick-Coupled Transcription/Translation System (Promega). Double-stranded DNAs were ^{32}P-labeled with [γ-^{32}P]ATP using T4 polynucleotide kinase and purified with NICK columns (GE Healthcare, Piscataway, NJ). ^{32}P-labeled double-stranded DNA for the human *HMGCS2* promoter region (P1, 5'-GTCTTTGACTCGCCCGTGTTCTGAGTGAGCCCTTTGACCCAGTTTTAGAAGCAGACTGAGCCACGGTG-3', corresponding to -147 to -79; P2, 5'-AGTGAGCCCTTTGACCCAGTT-3', corresponding to

Molecular Pharmacology Fast Forward. Published on September 5, 2020 as DOI: 10.1124/molpharm.120.000103
This article has not been copyedited and formatted. The final version may differ from this version.

-123 to -103) or a probe containing the DR5 motif of human *ABCG2* (5'-ATGTGACCCCTCCATGTACTTTC-3') (Benoki et al., 2012) were incubated with the in vitro synthesized proteins, and the reaction mixture was subjected to electrophoresis. The underlined probe sequences represent nuclear receptor binding motifs. Protein–DNA complexes were separated on 4% nondenaturing polyacrylamide gel. The radiation was detected by FLA-3000 image analyzer (FujiFilm, Tokyo, Japan).

DNA-affinity Assay

Biotin-labeled double-stranded DNA of *HMGCS2* promoter (-250 to +42) were incubated with in vitro synthesized hCAR, hPPARα and/or hRXRα proteins in the buffer containing 10 mM HEPES-KOH (pH 7.6), 0.1 M KCl, 3 mM $MgCl_2$, 0.1 mM EDTA, 10% glycerol and 1% NP-40 for 30 min at 4° C in the absence or presence of nonlabelled *HMGCS2* promoter (-250 to +42). Nuclear fraction of HepG2 cells was prepared by high-salt extraction method. Cells were homogenized in the lysis buffer containing 10 mM Hepes-KOH (pH7.6), 10 mM KCl, 1.5 mM $MgCl_2$, 1 mM dithiothreitol, 0.3% NP-40 and protease inhibitor cocktail and centrifuged. The pellets were resuspended with the lysis buffer supplemented with 0.1 mM EDTA, 10% glycerol and 325 mM NaCl and incubated on ice for 30 min. The suspensions were centrifuged at 20000 × g. Supernatant was dialyzed with the lysis buffer supplemented with 0.2 mM EDTA and 20% glycerol. The biotin-labeled DNA was precipitated by streptavidin magnetic beads (Invitrogen) and the precipitated complexes were eluted with SDS-PAGE sample buffer and subjected to Western blot analysis following the method reported previously (Shizu et al., 2018) with the antibodies indicated.

Pull-down Assay

Recombinant His-SUMO-CAR and His-SUMO-PPARα were prepared by following the method previously reported (Shizu et al., 2018). PGC1α was synthesized by a TNT SP6 High-Yield Wheat Germ Protein Expression System (Promega). His-SUMO-CAR and His-SUMO-PPARα were incubated on Ni-

Molecular Pharmacology Fast Forward. Published on September 5, 2020 as DOI: 10.1124/molpharm.120.000103
This article has not been copyedited and formatted. The final version may differ from this version.

NTA agarose (Qiagen, Valencia, CA) at 4°C for 1 h in buffer containing 20 mM Tris-HCl (pH 7.5), 0.5 mM EDTA, 1% Triton X-100, 10% glycerol and 100 mM NaCl. The agarose beads were washed with this buffer and incubated overnight with synthesized PGC1α in the buffer at 4°C. The precipitated complexes were eluted with SDS-PAGE sample buffer and subjected to Western blot analysis following the method reported previously (Shizu et al., 2018) with the indicated antibody.

Statistical Analysis

Statistical analyses were conducted with GraphPad Prism 7 (GraphPad Software, San Diego, CA). The significance of differences was assessed by Student's t-test for the comparison of data from two groups and one-way ANOVA followed by Dunnett's post hoc test or Bonferroni's correction for the comparison of multiple group data, which were considered appropriate based on the experimental design. Details of statistical analysis are given in the figure legend. *P*-values of less than 0.05 were regarded as statistically significant and asterisk are given on the comparisons. The values were not used for testing experimental hypotheses but are indicated to understand the differences between the compared groups. All experiments were repeated at least twice to confirm reproducibility. Sample sizes had been specified before conducting the experiment while the number of experiments to check the reproducibility was determined after the initial results were obtained.

Results:

CAR negatively regulates PPARα-dependent gene transcription in mouse liver and human hepatocytes.

First, to investigate the influence of CAR activation on the expression levels of energy metabolism-related genes related to lipid metabolism and insulin signals, a DNA microarray analysis was conducted with livers of the mice treated with the mouse CAR activator TCPOBOP for 5 consecutive days (Table S1) and the changes observed were confirmed by qRT-PCR for the genes related to insulin signaling, lipid metabolism and transcription factors. The genes with statistically significant changes are shown in Table 1. While TCPOBOP treatment increased the mRNA levels of *Pik3cb* and *Vldlr*, the treatment decreased

Molecular Pharmacology Fast Forward. Published on September 5, 2020 as DOI: 10.1124/molpharm.120.000103
This article has not been copyedited and formatted. The final version may differ from this version.

the expression of most of the PPARα target genes related to lipid metabolism (Bougarne et al., 2018) as well as insulin signal-related genes and some transcription factors, including PPARα itself. The results imply a functional interaction between CAR and PPARα, where CAR suppresses PPARα-dependent gene transcription.

To investigate the influence of CAR activation on PPARα target gene expression in human hepatocytes, cryopreserved human primary hepatocytes and human hepatocyte-like HepaRG cells were treated with CITCO, a human CAR activator, and mRNA levels of PPARα target genes were determined (Fig. 1). CITCO treatment obviously decreased the mRNA levels of *CPT1A*, *HMGCS2* and *CYP4A11* in human primary hepatocytes and those of *ACAT1*, *HMGCS2 and CYP4A11* in HepaRG cells. The treatment increased *CYP2B6*, a typical CAR target gene, in both cells. These results suggest that CAR activation decreases the expression of PPARα target genes also in human livers.

CAR functionally interacts with PPARα in mouse livers.

To investigate the functional interaction between CAR and PPARα on the gene transcription, mice were treated with TCPOBOP with or without the PPARα activator fenofibrate and the hepatic mRNA levels of PPARα target genes were determined (Fig. 2). As expected, the basal mRNA levels of the measured PPARα target genes related to lipid metabolism were decreased, or showed a tendency to decrease, upon treatment with TCPOBOP. Fenofibrate treatment increased these mRNA levels, but the upregulation was completely abolished by TCPOBOP cotreatment. TCPOBOP-mediated suppression of fenofibrate-induced expression was also observed for other PPARα target genes, namely, *G0s2*, *Vnn1*, *Pdk4* and *Gyk,* which are not associated with lipid metabolism, indicating the presence of a functional interaction between CAR and PPARα.

The influence of CAR activation on the regulation of lipid metabolism and PPARα target gene expression was also investigated using a different type of CAR activator, phenobarbital. Similar to the observation in epileptic patients, phenobarbital (1000 ppm) treatment increased blood TG levels 1.8-fold, and fenofibrate (1000 ppm) treatment decreased TG levels (Fig. 3A). The extent of phenobarbital-

Molecular Pharmacology Fast Forward. Published on September 5, 2020 as DOI: 10.1124/molpharm.120.000103
This article has not been copyedited and formatted. The final version may differ from this version.

dependent TG elevation was lower in the mice treated with fenofibrate than it was in the mice not treated with fenofibrate (Fig. 3A). Phenobarbital and/or fenofibrate treatment did not alter total cholesterol levels in blood under these experimental conditions in mice (data not shown).

As observed in Fig. 2, the mRNA levels of the PPARα target genes investigated were increased by fenofibrate treatment, and the upregulation was partially blocked by phenobarbital treatment (Fig. 3B). These changes were inversely correlated with the changes in blood TG levels. Similar results were observed in mice treated with lower doses of phenobarbital (300 ppm) and fenofibrate (300 ppm) for 1 week (Fig. S1). In these experiments, phenobarbital treatment decreased mRNA levels of PPARα target genes without decreasing that of *Ppara* (data not shown). These results suggest that CAR activation elevates blood TG levels by inhibiting the transcription of PPARα target genes.

CAR downregulates the expression of HMGCS2 gene*, a representative *PPARα target gene, through a PPARα-binding motif.

To investigate the mechanism for the CAR-mediated suppression of PPARα-dependent gene transcription, the HMGCS2 gene was used as a model gene for transcriptional analysis. Reporter assays were performed using constructs containing the ~6.8-kb promoter region of mouse *Hmgcs2* (Fig. 4A). Treatment with bezafibrate, a metabolism-independent PPARα activator (Hosaka et al., 2020; Willson et al., 2000), increased reporter activity, and the overexpression of CAR reduced it, depending on the amount expressed. The CAR-dependent suppression was much stronger with TCPOBOP treatment than it was without TCPOBOP. Similar results were observed with the human *HMGCS2* promoter and CITCO (Fig. 4B).

The rat *Hmgcs2* gene contains a peroxisome proliferator response element (PPRE) with a direct repeat 1 (DR1) sequence in its proximal promoter region (Rodriguez et al., 1994). We found that the element is conserved in both the human and mouse genes. We thus performed reporter assays with constructs containing ~250-bp proximal promoter regions containing a PPRE of mouse *Hmgcs2* or human *HMGCS2*. In line with the other experiments, the reporter activity was increased with bezafibrate treatment, and CAR

Molecular Pharmacology Fast Forward. Published on September 5, 2020 as DOI: 10.1124/molpharm.120.000103
This article has not been copyedited and formatted. The final version may differ from this version.

overexpression in combination treatment with its ligand blocked this bezafibrate-induced expression (Fig. 4C, 4D). The introduction of mutations into the PPRE (the DR1 motif) resulted in complete loss of bezafibrate-dependent induction and thereby CAR-mediated suppression of reporter activity (Fig. 4C, 4D). These results suggest that PPRE is necessary for CAR-mediated suppression of the expression of both mouse *Hmgcs2* and human *HMGCS2*.

To investigate the binding of the PPARα/RXRα heterodimer to the DR1 motif in the *HMGCS2* promoter and the effects of CAR on this binding, EMSAs were performed with two different lengths of oligo-DNAs containing the DR1 motif (Fig. 5A). Binding of the PPARα/RXRα heterodimer, but not CAR with or without RXRα, to both probes was confirmed, while the CAR/RXRα heterodimer was bound to the known CAR-binding motif, which was the DR5 motif in *ABCG2* (Benoki et al., 2012). The addition of excess CAR or RXRα had no effect on the binding of the PPARα/RXRα heterodimer to the DR1 motif (Fig. 5A, right). In addition, DNA-affinity assays were conducted with oligo-DNAs containing the DR1 motif (Fig. 5B). The PPARα/RXRα heterodimer was precipitated with the DR1 motif-containing bead, and this binding was competed with wild-type but not mutated DR1-containing oligo-DNA. Neither CAR monomer, CAR/RXRα heterodimer, nor PPARα monomer bound to the DR1 motif. These results suggest that CAR downregulates *HMGCS2* transcription without directly interacting with either the PPARα/RXRα heterodimer or its promoter region.

PGC1α is involved in the CAR-mediated suppression of PPARα.

Since CAR prevented PPARα-dependent transcription without inhibiting the binding of PPARα to PPRE, CAR might act on other cellular factor(s) involved in PPARα-dependent gene transcription in HepG2 cells. We therefore investigated the inhibitory effect of CAR in another cell line, African green monkey kidney-derived COS-1 cells. As shown in Fig. 4, CAR suppressed PPARα-activated transcription in the HepG2 cells (Fig. 6A); however, this CAR-mediated suppression was not observed in the COS-1 cells, although PPARα with bezafibrate treatment upregulated the PPRE-dependent reporter gene expression in this cell line (Fig. 6B). These results supported the idea that the cellular factor(s) highly expressed in

Molecular Pharmacology Fast Forward. Published on September 5, 2020 as DOI: 10.1124/molpharm.120.000103
This article has not been copyedited and formatted. The final version may differ from this version.

HepG2 cells but not COS-1 cells were important for the CAR-mediated suppression of PPARα function.

Since coactivators play key roles in the gene transcription mediated by both CAR and PPARα, they might be a target for the CAR-mediated suppression of PPARα function. To test this possibility, reporter assays were performed with wild-type and two different mutants of human CAR: CAR-ΔN, which lacks the N-terminal DBD and hinge region, and CAR-Δ8, which lacks 8 amino acids in the activation function 2 (AF2) domain required for coactivator recruitment (Fig. 6C). It was confirmed that these mutants had no ability to induce transcription through a CAR-binding motif since the expression of CAR-ΔN or CAR-Δ8 had no effect on the reporter activity in the assays using a reporter construct containing five tandem repeats of the NR1 motif from the *CYP2B6* promoter, which is known as a CAR-binding motif ($(NR1)_5$-tk-pGL3) (Fig. S2). In contrast, CAR-ΔN, but not CAR-Δ8, inhibited PPARα-dependent reporter gene activation, as did wild-type CAR (Fig. 6C), suggesting that the AF2 domain, but not DBD or the hinge region, is necessary for CAR-mediated suppression of PPARα function.

To further investigate the role of coactivators in the CAR-mediated suppression of PPARα-dependent gene transcription, we sought coactivator(s) crucial for CAR- and PPARα-mediated transactivation. Among the several coactivators associated with CAR and PPARα, the expression of PGC1α exhibited the highest activity in both CAR- and PPARα-dependent transcription when $(NR1)_5$-tk-pGL3 and HMGCS2-250bp-Luc were transfected, respectively (Fig. 7A, 7B). As expected, the CAR-Δ8-expressing cells showed no transcriptional activation even in the presence of coactivators, including PGC1α (Fig. 7A). Finally, PGC1α mRNA levels were found to be 40-fold higher in HepG2 cells than they were in COS-1 cells (Fig. 7C). Taken together, these findings suggest that PGC1α is a key coactivator for the functional interaction between CAR and PPARα.

Next, the influence of PGC1α overexpression on the CAR-mediated suppression of PPARα-induced *HMGCS2* expression was examined in reporter assays with COS-1 cells. PGC1α overexpression increased reporter activity, and this increase was abolished by the coexpression of wild-type CAR upon CITCO treatment (Fig. 8A). This suppressive effect was also observed with CAR-ΔN but not with CAR-Δ8 (Fig. 8A). Moreover, cotreatment of the cells with PGC1α inhibitor SR18292 (Sharabi et al., 2017) attenuated

Molecular Pharmacology Fast Forward. Published on September 5, 2020 as DOI: 10.1124/molpharm.120.000103
This article has not been copyedited and formatted. The final version may differ from this version.

the PPARα- and PGC1α-induced expression of the reporter gene and completely blocked CAR-mediated repression (Fig. 8B). Consistently, siRNA-dependent repression of PGC1α expression in HepG2 cells attenuated PPARα-mediated transcription and its suppression by CAR (Fig. 8C). These results corroborate the possible involvement of PGC1α in the CAR-mediated suppression of PPARα-induced *HMGCS2* transcription.

CAR competes with PPARα for PGC1α binding.

To determine the interaction between PGC1α and CAR or PPARα, mammalian two-hybrid assays were performed. The nuclear receptor-interacting LXXLL motif in PGC1α was fused with GAL4-DBD (GAL4-PGC1α), and it was coexpressed with VP16 transactivation domain-fused CAR or PPARα. As shown in Fig. 9A, coexpression increased luciferase activity, indicating that both CAR and PPARα interacted with the LXXLL motif derived from PGC1α. In contrast, CAR-Δ8 did not interact with the motif as expected (Fig. 9A). When the LXXLL motif of GRIP1 was used, no interaction with CAR or PPARα was observed (data not shown).

Next, to determine the influence of CAR expression on the interaction between PPARα and PGC1α, wild-type CAR or the CAR-Δ8 mutant was coexpressed with VP16-PPARα and GAL4-PGC1α (Fig. 9B). The interaction between VP16-PPARα and GAL4-PGC1α, indicated by detected luciferase activity, was abolished by the expression of wild-type CAR but not CAR-Δ8 (Fig. 9B). Pull-down assays with recombinant CAR and PPARα proteins with *in vitro* synthesized PGC1α confirmed the interactions between CAR and PGC1α and between PPARα and PGC1α and demonstrated that the interaction between CAR and PGC1α was stronger than that between PPARα and PGC1α (Fig. S3). These results suggest that CAR competes with PPARα for PGC1α binding by inhibiting the PPARα-PGC1α interaction.

PGC1α is involved in CAR-mediated TG elevation in vivo

Finally, to determine the influence of PGC1α inhibition with the chemical inhibitor SR18292 (Sharabi et al., 2017) on CAR-mediated TG elevation and the expression of PPARα target genes *in vivo*, mice were

Molecular Pharmacology Fast Forward. Published on September 5, 2020 as DOI: 10.1124/molpharm.120.000103
This article has not been copyedited and formatted. The final version may differ from this version.

cotreated with phenobarbital and SR18292. As shown in Fig. 10A, the SR18292 treatment diminished the phenobarbital-dependent increase in plasma TG levels. The SR18292 treatment also attenuated phenobarbital-dependent downregulation of PPARα target genes *Acat1* and *Hmgcs2*, although it did not affect that of *Acox1* or *Cpt1a* (Fig. 10B).These results suggest that PGC1α plays a role in the phenobarbital-induced inhibition of PPARα target gene expression and the resulting increase in blood TG levels.

Discussion:

Elevation of blood TG levels is sometimes observed with enzyme-inducing AED treatment. Since drug-metabolizing enzyme induction by AEDs is mediated mainly by CAR, this receptor was expected to be a key factor for the blood TG elevation induced by AED treatment. On the other hand, PPARα is known as an important factor for lipid metabolism (Bougarne et al., 2018), and fibrates lower blood TG levels via PPARα activation (Bougarne et al., 2018). A recent report demonstrated that TCPOBOP treatment increased blood TG levels and decreased the expression of PPARα target genes, *Cyp4a14* and *Cpt1a*, in wild-type but not in *Car*$^{-/-}$ mice (Maglich et al., 2009), but the mechanism remained to be investigated. In this study, the results obtained in *in vitro* and *in vivo* studies suggest that CAR inhibits PPARα-dependent gene transcription, which might lead to the elevation of plasma TG levels.

Using a DNA microarray and qRT-PCR analyses with the livers of mice treated with TCPOBOP, we found that the expression levels of the genes related to lipid metabolism and insulin signals were altered by CAR activation. In particular, CAR downregulated the genes involved in fatty acid oxidation, which are PPARα target genes (Bougarne et al., 2018). The fenofibrate-induced expression of hepatic PPARα target genes in mice was attenuated by TCPOBOP or phenobarbital treatment. Reporter assays, mammalian two-hybrid assays and DNA affinity assays revealed that CAR could prevent PPARα from recruiting PGC1α for gene transcription.

Although it is well known that the blood TG-lowering effects of fibrates are PPARα-dependent, key PPARα target genes directly associated with the pharmacological effects are still controversial. In this

Molecular Pharmacology Fast Forward. Published on September 5, 2020 as DOI: 10.1124/molpharm.120.000103
This article has not been copyedited and formatted. The final version may differ from this version.

study, we carried out the experiments focusing on representative PPARα target genes, which are not necessarily demonstrated as direct targets of TG-lowering. However, we have demonstrated that CAR-dependent suppression of PPARα functions is not limited to lipid metabolism-related genes but is common to various PPARα target genes. In addition, treatment of mice with the PGC1α inhibitor SR18292 prevented the phenobarbital-dependent elevation of blood TG levels. Therefore, the mechanism proposed in this study might explain, at least in part, the observation of enzyme-inducing AED-dependent blood TG elevation.

Our findings on CAR-mediated inhibition of PPARα target gene expression are consistent with previous reports. It has been reported that CAR activation decreases the expression of genes related to fatty acid oxidation, such as *Cpt1a* (Rezen et al., 2009), and that CAR prevents PPARα activation-dependent signaling in the liver (Kassam et al., 2000; Li et al., 2016). In a study reported by Kassam et al., CAR was directly bound to a PPRE in the promoter of the gene encoding 3-hydroxyacyl-CoA dehydrogenase, an enzyme involved in fatty acid β-oxidation, and inhibited PPARα binding to the motif and its gene transcription (Kassam et al., 2000). In contrast, our present results suggest that CAR prevents PPARα-dependent transcription of genes related to fatty acid metabolism by competing with PPARα for PGC1α binding without directly binding to the PPRE in the promoter of *HMGCS2*. Therefore, CAR may prevent PPARα-dependent gene transcription through several mechanisms, depending on the target gene.

CAR activation downregulated the expression of PPARα target genes in both mouse livers and human hepatocytes, although the extent of this downregulation varied among genes. Moreover, in reporter assays using promoter regions from mouse and human *HMGCS2* genes, which contain a conserved PPRE motif, CAR inhibited both human and mouse PPARα-dependent gene transcription. Although some functions of CAR, such as liver cancer promotion (Shizu and Yoshinari, 2020; Wang et al., 2012), have been observed to differ by species, our current results suggest that CAR-mediated regulation of energy metabolism through the inhibition of PPARα/PGC1α may be a common system across various species.

We observed that CAR competed with PPARα for PGC1α binding. Competition for a coactivator among CAR and other receptors has been previously reported: CAR prevents hepatocyte nuclear factor 4α

Molecular Pharmacology Fast Forward. Published on September 5, 2020 as DOI: 10.1124/molpharm.120.000103
This article has not been copyedited and formatted. The final version may differ from this version.

(HNF4α)-dependent transactivation by competing for interactions with coactivators GRIP1 and PGC1α (Miao et al., 2006) and estrogen receptor-dependent gene transcription through competition for GRIP1 binding (Min et al., 2002b). Moreover, wild-type CAR but not the AF2-lacking mutant prevented the transcription of human *APOA1* through a DR1 motif, suggesting the involvement of coactivators in this inhibition (Masson et al., 2008). Since CAR shares coactivators with many nuclear receptors, including PPARα, CAR activation may attenuate gene expression via these nuclear receptors.

It is known that there are two types of CAR activators; direct ligands, such as TCPOBOP and CITCO, and indirect activators, such as phenobarbital (Negishi, 2017). The present results suggest that the CAR-dependent regulation of PPARα and blood TG levels involves the competition of PGC1α, which occurs in nucleus after CAR activation. We thus assume it is indicated that CAR activated by either type of activator regulates the blood TG levels through the same mechanism.

Gene transcription by nuclear receptor pregnane X receptor (PXR, NR1I2), which is similar to CAR, is also activated by PGC1α and GRIP1 (Okamura et al., 2019), indicating that PXR activation likely prevents PPARα-dependent transcription in a manner similar to CAR-induced inhibition. A report suggested that PXR prevents HNF4α-dependent gene transcription by competing for PGC1α binding (Bhalla et al., 2004). In fact, our preliminary study demonstrated that PXR attenuated the interaction between PPARα and PGC1α and inhibited gene transcription by PPARα (data not shown). Since CAR and PXR are involved in various physiological events in the liver (Banerjee et al., 2015), further studies are needed to determine the role of cross talk between these xenobiotic-responsive receptors and among other nuclear receptors in liver function and diseases.

In this study, we have demonstrated that CAR controls the expression of energy metabolism-related genes through the attenuation of PPARα and PGC1α function. PGC1α and PPARα are vital factors for maintaining energy metabolism (Kersten et al., 1999; Liang and Ward, 2006; Sengupta et al., 2010; Yoon et al., 2001). The expression of PGC1α and PPARα is increased by fasting, which upregulates gluconeogenesis, mitochondrial biogenesis and fatty acid oxidation (Kersten et al., 1999; Liang and Ward, 2006; Sengupta et al., 2010; Yoon et al., 2001). In addition, the expression level and transcriptional

Molecular Pharmacology Fast Forward. Published on September 5, 2020 as DOI: 10.1124/molpharm.120.000103
This article has not been copyedited and formatted. The final version may differ from this version.

activity of CAR is upregulated in fasting animals, and this induction is dependent on fasting-activated PGC1α (Ding et al., 2006). On the other hand, PPARα activation in mice or rats induces the expression and activation of CAR (Guo et al., 2007; Lu et al., 2011; Rakhshandehroo et al., 2010; Saito et al., 2010; Wieneke et al., 2007), and fasting-dependent CAR induction is attenuated in PPARα-deficient mice (Wieneke et al., 2007). Taken together, the results from our study and those from other groups suggest that CAR plays a role as a part of the energy homeostasis system in cooperation with PPARα and PGC1α, where CAR expression is regulated by PPARα and PGC1α and CAR regulates PPARα/PGC1α-dependent gene transcription.

In conclusion, we have revealed the molecular mechanism by which CAR mediates the inhibition of PPARα-dependent gene transcription as related to blood TG control, providing a new insight into the side effects of enzyme-inducing AEDs, such as phenobarbital and carbamazepine. The molecular mechanism involves competition between nuclear receptors for coactivator PGC1α binding. Since almost all nuclear receptors utilize common coactivators, other nuclear receptor combinations, in addition to CAR and PPARα, may compete for coactivator interaction and be involved in various biological phenomena.

Authorship Contributions:

Participated in research design: Shizu, Otsuka, Ezaki, Abe, Yoshinari.

Conducted experiments: Shizu, Otsuka, Ezaki, Ishii, Arakawa, Amaike, Abe, Hosaka.

Performed data analysis: Shizu, Otsuka, Ezaki, Ishii, Arakawa, Amaike, Abe, Hosaka, Sasaki, Miyata, Yamazoe, Yoshinari.

Wrote or contribute to the writing of the paper: Shizu, Otsuka, Ezaki, Arakawa, Abe, Hosaka, Kanno, Yoshinari.

Conflict of Interest: The authors declare that they have no conflicts of interest with contents of this article.

Molecular Pharmacology Fast Forward. Published on September 5, 2020 as DOI: 10.1124/molpharm.120.000103
This article has not been copyedited and formatted. The final version may differ from this version.

References:

Abe T, Amaike Y, Shizu R, Takahashi M, Kano M, Hosaka T, Sasaki T, Kodama S, Matsuzawa A and Yoshinari K (2018) Role of YAP Activation in Nuclear Receptor CAR-Mediated Proliferation of Mouse Hepatocytes. *Toxicol Sci* **165**(2): 408-419.

Banerjee M, Robbins D and Chen T (2015) Targeting xenobiotic receptors PXR and CAR in human diseases. *Drug Discov Today* **20**(5): 618-628.

Benoki S, Yoshinari K, Chikada T, Imai J and Yamazoe Y (2012) Transactivation of ABCG2 through a novel cis-element in the distal promoter by constitutive androstane receptor but not pregnane X receptor in human hepatocytes. *Arch Biochem Biophys* **517**(2): 123-130.

Berger J and Moller DE (2002) The Mechanisms of Action of PPARs. *Annual Review of Medicine* **53**(1): 409-435.

Berlit P, Krause KH, Heuck CC and Schellenberg B (1982) Serum lipids and anticonvulsants. *Acta Neurol Scand* **66**(3): 328-334.

Bhalla S, Ozalp C, Fang S, Xiang L and Kemper JK (2004) Ligand-activated pregnane X receptor interferes with HNF-4 signaling by targeting a common coactivator PGC-1alpha. Functional implications in hepatic cholesterol and glucose metabolism. *J Biol Chem* **279**(43): 45139-45147.

Bougarne N, Weyers B, Desmet SJ, Deckers J, Ray DW, Staels B and De Bosscher K (2018) Molecular Actions of PPARα in Lipid Metabolism and Inflammation. *Endocr Rev* **39**(5): 760-802.

Chen NC, Chen CH, Lin TK, Chen SD, Tsai MH, Chang CC, Tsai WC and Chuang YC (2018) Risk of Microangiopathy in Patients with Epilepsy under Long-term Antiepileptic Drug Therapy. *Front Neurol* **9**: 113.

Chuang YC, Chuang HY, Lin TK, Chang CC, Lu CH, Chang WN, Chen SD, Tan TY, Huang CR and Chan SH (2012) Effects of long-term antiepileptic drug monotherapy on vascular risk factors and atherosclerosis. *Epilepsia* **53**(1): 120-128.

Ding X, Lichti K, Kim I, Gonzalez FJ and Staudinger JL (2006) Regulation of constitutive androstane receptor and its target genes by fasting, cAMP, hepatocyte nuclear factor alpha, and the

coactivator peroxisome proliferator-activated receptor gamma coactivator-1alpha. *J Biol Chem* **281**(36): 26540-26551.

Dong B, Saha PK, Huang W, Chen W, Abu-Elheiga LA, Wakil SJ, Stevens RD, Ilkayeva O, Newgard CB, Chan L and Moore DD (2009) Activation of nuclear receptor CAR ameliorates diabetes and fatty liver disease. *Proc Natl Acad Sci U S A* **106**(44): 18831-18836.

Gao J, He J, Zhai Y, Wada T and Xie W (2009) The constitutive androstane receptor is an anti-obesity nuclear receptor that improves insulin sensitivity. *J Biol Chem* **284**(38): 25984-25992.

Guo D, Sarkar J, Suino-Powell K, Xu Y, Matsumoto K, Jia Y, Yu S, Khare S, Haldar K, Rao MS, Foreman JE, Monga SP, Peters JM, Xu HE and Reddy JK (2007) Induction of nuclear translocation of constitutive androstane receptor by peroxisome proliferator-activated receptor alpha synthetic ligands in mouse liver. *J Biol Chem* **282**(50): 36766-36776.

Hosaka T, Wakatsuki A, Sasaki T, Shizu R and Yoshinari K (2020) Construction of a PPARα Reporter Assay System with Drug-Metabolizing Capability. *BPB Reports* **3**(1): 7-10.

Isojarvi JI, Pakarinen AJ and Myllyla VV (1993) Serum lipid levels during carbamazepine medication. A prospective study. *Arch Neurol* **50**(6): 590-593.

Kassam A, Winrow CJ, Fernandez-Rachubinski F, Capone JP and Rachubinski RA (2000) The peroxisome proliferator response element of the gene encoding the peroxisomal beta-oxidation enzyme enoyl-CoA hydratase/3-hydroxyacyl-CoA dehydrogenase is a target for constitutive androstane receptor beta/9-cis-retinoic acid receptor-mediated transactivation. *J Biol Chem* **275**(6): 4345-4350.

Kersten S, Seydoux J, Peters JM, Gonzalez FJ, Desvergne B and Wahli W (1999) Peroxisome proliferator-activated receptor alpha mediates the adaptive response to fasting. *J Clin Invest* **103**(11): 1489-1498.

Li CY, Cheng SL, Bammler TK and Cui JY (2016) Neonatal Activation of the Xenobiotic-Sensors PXR and CAR Results in Acute and Persistent Down-regulation of PPARalpha-Signaling in Mouse Liver. *Toxicol Sci* **153**(2): 282-302.

Liang H and Ward WF (2006) PGC-1α: a key regulator of energy metabolism. *Advances in Physiology*

Education **30**(4): 145-151.

Livingston S (1976) Letter: Phenytoin and serum cholesterol. *Br Med J* **1**(6009): 586.

Lu Y, Boekschoten MV, Wopereis S, Muller M and Kersten S (2011) Comparative transcriptomic and metabolomic analysis of fenofibrate and fish oil treatments in mice. *Physiol Genomics* **43**(23): 1307-1318.

Maglich JM, Lobe DC and Moore JT (2009) The nuclear receptor CAR (NR1I3) regulates serum triglyceride levels under conditions of metabolic stress. *J Lipid Res* **50**(3): 439-445.

Masson D, Qatanani M, Sberna AL, Xiao R, Pais de Barros JP, Grober J, Deckert V, Athias A, Gambert P, Lagrost L, Moore DD and Assem M (2008) Activation of the constitutive androstane receptor decreases HDL in wild-type and human apoA-I transgenic mice. *J Lipid Res* **49**(8): 1682-1691.

Miao J, Fang S, Bae Y and Kemper JK (2006) Functional inhibitory cross-talk between constitutive androstane receptor and hepatic nuclear factor-4 in hepatic lipid/glucose metabolism is mediated by competition for binding to the DR1 motif and to the common coactivators, GRIP-1 and PGC-1alpha. *J Biol Chem* **281**(21): 14537-14546.

Min G, Kemper JK and Kemper B (2002a) Glucocorticoid receptor-interacting protein 1 mediates ligand-independent nuclear translocation and activation of constitutive androstane receptor in vivo. *J Biol Chem* **277**(29): 26356-26363.

Min G, Kim H, Bae Y, Petz L and Kemper JK (2002b) Inhibitory cross-talk between estrogen receptor (ER) and constitutively activated androstane receptor (CAR). CAR inhibits ER-mediated signaling pathway by squelching p160 coactivators. *J Biol Chem* **277**(37): 34626-34633.

Mintzer S, Skidmore CT, Abidin CJ, Morales MC, Chervoneva I, Capuzzi DM and Sperling MR (2009) Effects of antiepileptic drugs on lipids, homocysteine, and C-reactive protein. *Annals of Neurology* **65**(4): 448-456.

Negishi M (2017) Phenobarbital Meets Phosphorylation of Nuclear Receptors. *Drug Metabolism and Disposition* **45**(5): 532-539.

Okamura M, Shizu R, Hosaka T, Sasaki T and Yoshinari K (2019) Possible involvement of the competition for the transcriptional coactivator glucocorticoid receptor-interacting protein 1 in the

inflammatory signal-dependent suppression of PXR-mediated CYP3A induction in vitro. *Drug Metab Pharmacokinet* **34**(4): 272-279.

Rakhshandehroo M, Knoch B, Muller M and Kersten S (2010) Peroxisome proliferator-activated receptor alpha target genes. *PPAR Res* **2010**: 612089.

Rezen T, Tamasi V, Lovgren-Sandblom A, Bjorkhem I, Meyer UA and Rozman D (2009) Effect of CAR activation on selected metabolic pathways in normal and hyperlipidemic mouse livers. *BMC Genomics* **10**: 384.

Rodriguez JC, Gil-Gomez G, Hegardt FG and Haro D (1994) Peroxisome proliferator-activated receptor mediates induction of the mitochondrial 3-hydroxy-3-methylglutaryl-CoA synthase gene by fatty acids. *J Biol Chem* **269**(29): 18767-18772.

Roth A, Looser R, Kaufmann M, Blattler SM, Rencurel F, Huang W, Moore DD and Meyer UA (2008) Regulatory cross-talk between drug metabolism and lipid homeostasis: constitutive androstane receptor and pregnane X receptor increase Insig-1 expression. *Mol Pharmacol* **73**(4): 1282-1289.

Saito K, Kobayashi K, Mizuno Y, Fukuchi Y, Furihata T and Chiba K (2010) Peroxisome proliferator-activated receptor alpha (PPARalpha) agonists induce constitutive androstane receptor (CAR) and cytochrome P450 2B in rat primary hepatocytes. *Drug Metab Pharmacokinet* **25**(1): 108-111.

Sengupta S, Peterson TR, Laplante M, Oh S and Sabatini DM (2010) mTORC1 controls fasting-induced ketogenesis and its modulation by ageing. *Nature* **468**(7327): 1100-1104.

Sharabi K, Lin H, Tavares CDJ, Dominy JE, Camporez JP, Perry RJ, Schilling R, Rines AK, Lee J, Hickey M, Bennion M, Palmer M, Nag PP, Bittker JA, Perez J, Jedrychowski MP, Ozcan U, Gygi SP, Kamenecka TM, Shulman GI, Schreiber SL, Griffin PR and Puigserver P (2017) Selective Chemical Inhibition of PGC-1alpha Gluconeogenic Activity Ameliorates Type 2 Diabetes. *Cell* **169**(1): 148-160.

Shiraki T, Sakai N, Kanaya E and Jingami H (2003) Activation of orphan nuclear constitutive androstane receptor requires subnuclear targeting by peroxisome proliferator-activated receptor gamma coactivator-1 alpha. A possible link between xenobiotic response and nutritional state. *J Biol Chem* **278**(13): 11344-11350.

Shizu R, Min J, Sobhany M, Pedersen LC, Mutoh S and Negishi M (2018) Interaction of the phosphorylated DNA-binding domain in nuclear receptor CAR with its ligand-binding domain regulates CAR activation. *J Biol Chem* **293**(1): 333-344.

Shizu R and Yoshinari K (2020) Nuclear receptor CAR-mediated liver cancer and its species differences. *Expert Opin Drug Metab Toxicol* **16**(4): 343-351.

Sueyoshi T, Kawamoto T, Zelko I, Honkakoski P and Negishi M (1999) The repressed nuclear receptor CAR responds to phenobarbital in activating the human CYP2B6 gene. *J Biol Chem* **274**(10): 6043-6046.

Svalheim S, Luef G, Rauchenzauner M, Mørkrid L, Gjerstad L and Taubøll E (2010) Cardiovascular risk factors in epilepsy patients taking levetiracetam, carbamazepine or lamotrigine. *Acta Neurologica Scandinavica* **122**(s190): 30-33.

Tan TY, Lu CH, Chuang HY, Lin TK, Liou CW, Chang WN and Chuang YC (2009) Long-term antiepileptic drug therapy contributes to the acceleration of atherosclerosis. *Epilepsia* **50**(6): 1579-1586.

Timsit YE and Negishi M (2007) CAR and PXR: the xenobiotic-sensing receptors. *Steroids* **72**(3): 231-246.

Verrotti A, Basciani F, Domizio S, Sabatino G, Morgese G and Chiarelli F (1998) Serum lipids and lipoproteins in patients treated with antiepileptic drugs. *Pediatr Neurol* **19**(5): 364-367.

Wada T, Gao J and Xie W (2009) PXR and CAR in energy metabolism. *Trends Endocrinol Metab* **20**(6): 273-279.

Wang Y-M, Ong SS, Chai SC and Chen T (2012) Role of CAR and PXR in xenobiotic sensing and metabolism. *Expert Opin Drug Metab Toxicol* **8**(7): 803-817.

Wei P, Zhang J, Egan-Hafley M, Liang S and Moore DD (2000) The nuclear receptor CAR mediates specific xenobiotic induction of drug metabolism. *Nature* **407**(6806): 920-923.

Wieneke N, Hirsch-Ernst KI, Kuna M, Kersten S and Puschel GP (2007) PPARalpha-dependent induction of the energy homeostasis-regulating nuclear receptor NR1i3 (CAR) in rat hepatocytes: potential role in starvation adaptation. *FEBS Lett* **581**(29): 5617-5626.

Willson TM, Brown PJ, Sternbach DD and Henke BR (2000) The PPARs: from orphan receptors to drug discovery. *J Med Chem* **43**(4): 527-550.

Yoon JC, Puigserver P, Chen G, Donovan J, Wu Z, Rhee J, Adelmant G, Stafford J, Kahn CR, Granner DK, Newgard CB and Spiegelman BM (2001) Control of hepatic gluconeogenesis through the transcriptional coactivator PGC-1. *Nature* **413**(6852): 131-138.

Yoshinari K, Yoda N, Toriyabe T and Yamazoe Y (2010) Constitutive androstane receptor transcriptionally activates human CYP1A1 and CYP1A2 genes through a common regulatory element in the 5'-flanking region. *Biochem Pharmacol* **79**(2): 261-269.

Zeitlhofer J, Doppelbauer A, Tribl G, Leitha T and Deecke L (1993) Changes of serum lipid patterns during long-term anticonvulsive treatment. *Clin Investig* **71**(7): 574-578.

Molecular Pharmacology Fast Forward. Published on September 5, 2020 as DOI: 10.1124/molpharm.120.000103
This article has not been copyedited and formatted. The final version may differ from this version.

Footnote:

This study was supported in part by a Grant-in-Aid from Ministry of Education, Culture, Sports, Sciences and Technology of Japan [22390027, 17K08418, 20K07202] and a grant from the Japan Chemical Industry Association (JCIA) Long-range Research Initiative (LRI).

Legends:

Fig. 1. Influence of CAR activation on the expression levels of PPARα target genes in human primary hepatocytes and HepaRG cells.

Cryopreserved human hepatocytes (Lot. HEP187111: White 56-year-old female, A) or HepaRG cells (B) were treated with CITCO (1 μM) for 48 hours. Total RNA was extracted and subjected to qRT-PCR to determine PPARα and CAR target genes indicated. The mRNA levels of the indicated genes were normalized to those of *GAPDH.* Data are shown as the means ± S. D. with the plots of individual sample data (n = 4). Differences between the responses of CITCO were determined by Student's *t*-test (**p* < 0.05).

.

Fig. 2. Influence of TCPOBOP treatment on the expression levels of PPARα target genes in the liver of the fenofibrate-treated mice.

Mice were treated with 300 ppm fenofibrate and/or 3 mg/kg TCPOBOP as described under the Experimental procedures. Hepatic mRNA levels of the indicated PPARα target genes were determined by qRT-PCR. The mRNA levels of the indicated target genes were normalized to those of *Actb.* Data are shown as the means ± S. D. with the plots of individual mouse data (n = 3-4). Differences in response among the groups were tested by one-way ANOVA. Differences between the indicated combinations were determined with Bonferroni's correction (**p* < 0.05; NS, not significant).

Fig. 3. Influence of phenobarbital treatment on plasma TG levels and the expression of PPARα target genes in the liver of the fenofibrate-treated mice.

Molecular Pharmacology Fast Forward. Published on September 5, 2020 as DOI: 10.1124/molpharm.120.000103
This article has not been copyedited and formatted. The final version may differ from this version.

Mice were treated with 1000 ppm fenofibrate and/or 1000 ppm phenobarbital (PB) for one week. (A) Plasma TG concentrations were determined with a commercial kit. (B) mRNA levels of PPARα target genes were determined by qRT-PCR. The mRNA levels of the indicated target genes were normalized to those of *Actb*. Data are shown as the mean ± S. D. with the plots of individual mouse data (n = 5). Differences in response among the groups were tested by one-way ANOVA. Differences between the indicated combinations were determined by Bonferroni's correction (*$p < 0.05$; NS, not significant).

Fig. 4. Influence of CAR activation on the PPARα-mediated gene transcription of mouse *Hmgcs2* and human *HMGCS2*.

(A, B) HepG2 cells were transfected with reporter constructs including -6779 to +33 of mouse *Hmgcs2* or -6784 to +42 of human *HMGCS2* (250 ng) in the presence or absence of various amounts of mouse CAR (mCAR)- or human CAR (hCAR)-expressing plasmids (0.5, 5, 50 ng). The cells were treated with vehicle (0.2% DMSO), bezafibrate (BZF, 100 μM), and/or TCPOBOP (250 nM) or CITCO (1 μM) for 24 h, and reporter activity was determined. Data are shown as the mean ± S. D. with the plots of individual sample data (n = 4). (C, D) HepG2 cells were transfected with the expression plasmid for mCAR or hCAR (50 ng) and a reporter plasmid containing the -250 to +33 sequence of mouse *Hmgcs2* or the -250 to +42 sequence of human *HMGCS2* (250 ng). The cells were then treated with vehicle (0.2% DMSO), bezafibrate (BZF, 100 μM), and/or TCPOBOP (250 nM) or CITCO (1 μM) for 24 h, and the reporter activity was determined. Closed and open circles in the left panel represent wild-type and mutated DR1 (PPRE) motifs, respectively. Data are shown as the means ± S. D. (n = 4). Differences in response among the groups were tested by one-way ANOVA. Differences between the indicated combinations were determined by Bonferroni's correction (*$p < 0.05$).

Fig. 5. The binding of PPARα and CAR to the *HMGCS2* promoter.

(A) EMSAs were performed with two ^{32}P-labeled human *HMGCS2*-derived double-stranded DNA and a probe containing the DR5 motif from human *ABCG2,* and *in vitro* synthesized nuclear receptor proteins.

Molecular Pharmacology Fast Forward. Published on September 5, 2020 as DOI: 10.1124/molpharm.120.000103
This article has not been copyedited and formatted. The final version may differ from this version.

The labels “x2” and “x4” indicate that 2-fold and 4-fold higher amount, respectively, of the synthesized proteins were added compared to the control samples. (B) DNA-affinity assays were performed with *in vitro* synthesized nuclear receptor proteins and biotin-labeled DNA derived from the *HMGCS2* promoter (-250 to +42). Wild-type or mutated (as in Fig. 4D) nonlabelled oligo-DNA were added to the reactions in upper and middle panels. In the bottom, the nuclear extract prepared from HepG2 cells was included in the reaction samples. Eluates (E), unbound (U) fractions and input (I) samples were subjected to immunoblotting with anti-PPARα or anti-V5 antibody. The EMSA and DNA-affinity assays were repeated more than three times and confirmed the reproducibility.

Fig. 6. The difference in the CAR-mediated suppression of *HMGCS2* in HepG2 and COS-1 cells.
(A, B) Reporter gene assays were performed in HepG2 (A) or COS-1 cells (B) with the reporter construct containing the -250 to +42 sequence of human *HMGCS2* (HMGCS2-250bp-Luc, 10 ng) and the plasmid expressing hCAR (0.5, 5 or 50 ng) and/or hPPARα (10 ng), as indicated. The cells were treated with CITCO (1 μM) and/or bezafibrate (BZF, 100 μM) for 24 h. Then, the reporter activity was determined. Data are shown as the means ± S. D. (n = 4). (C) Reporter gene assays were conducted in HepG2 cells with HMGCS2-250bp-Luc (10 ng), the expression plasmid for CAR-WT, CAR-ΔN (ΔN), CAR-Δ8 (Δ8) (50 ng) and/or PPARα (10 ng). The cells were treated with vehicle (0.2% DMSO), CITCO (1 μM) and/or BZF (100 μM) for 24 h, and the reporter activity was determined. Data are shown as the means ± S. D. (n=4). Differences in response among the groups were tested by one-way ANOVA. Differences between the indicated combinations were determined by Bonferroni’s correction (*$p < 0.05$; NS, not significant).

Fig. 7. Identification of a coactivator that activates CAR- and PPARα-mediated gene transcription.
(A, B) Reporter gene assays were conducted in COS-1 cells with $(NR1)_5$-tk-pGL3 (20 ng) and the expression plasmid for CAR-WT or CAR-Δ8 (20 ng) (A) or HMGCS2-250bp-Luc (20 ng) and the expression plasmid for PPARα (20 ng) (B), in combination with a series of pFN21A plasmids (40 ng) harboring coactivator cDNA as indicated. The cells were treated with vehicle (0.1% DMSO), CITCO (1

Molecular Pharmacology Fast Forward. Published on September 5, 2020 as DOI: 10.1124/molpharm.120.000103
This article has not been copyedited and formatted. The final version may differ from this version.

μM) (A) or bezafibrate (BZF, 100 μM) (B) for 24 h, and the reporter activity was determined. Data are shown as the means ± S. D. with the plots of individual sample data (n=4). (C) *PGC1α* mRNA levels in the COS-1 cells and HepG2 cells were determined by qRT-PCR. The *PGC1α* mRNA levels were normalized to those of *GAPDH,* and the relative mRNA level in the COS-1 cells was set at 1. Data are shown as the means ± S. D. (n=4) with the plots of individual sample data.

Fig. 8. The role of PGC1α in the CAR-mediated downregulation of PPARα.

(A) Reporter gene assays were conducted in COS-1 cells with HMGCS2-250bp-Luc (10 ng), the expression plasmid for CAR-WT, CAR-ΔN (ΔN), CAR-Δ8 (Δ8) (50 ng), PPARα (10 ng) or PGC1α (50 ng) as indicated. The cells were treated with vehicle (0.2% DMSO), CITCO (1 μM) and/or bezafibrate (BZF, 100 μM) for 24 h, and the reporter activity was determined. Data are shown as the means ± S. D. (n=4). Differences in response among the groups were tested by one-way ANOVA. Differences between the indicated combinations were determined by Bonferroni's correction (*$p < 0.05$; NS, not significant). (B) Reporter gene assays were conducted in COS-1 cells with HMGCS2-250bp-Luc (10 ng), the expression plasmid for CAR (50 ng), PPARα (10 ng) and/or PGC1α (50 ng), and phRL-CMV (10 ng) as indicated. After 24 h in culture, the cells were treated with vehicle (0.3% DMSO), bezafibrate (BZF, 100 μM), CITCO (1 μM), and/or SR18292 (30 μM) for 24 h, and the reporter activity was determined. Data are shown as the means ± S. D. (n=4). Differences in response among the groups were tested by one-way ANOVA. Differences between the indicated combinations were determined by Bonferroni's correction (*$p < 0.05$; NS, not significant). (C) Reporter gene assays were conducted in HepG2 cells with siRNA targeting PGC1α (10 nM) or control siRNA and 48 h later transfected with HMGCS2-250bp-Luc (10 ng) and the expression plasmid for CAR (50 ng) and/or PPARα (10 ng) and phRL-SV40 (10 ng). The Cells were treated with vehicle (0.2% DMSO), bezafibrate (BZF, 100 μM) and/or CITCO (1 μM) for 24 h, and the reporter activity was determined. Data are shown as the means ± S. D. (n=4). Differences in response among the groups were tested by one-way ANOVA. Differences between the indicated combinations were determined by Bonferroni's correction (*$p < 0.05$).

Molecular Pharmacology Fast Forward. Published on September 5, 2020 as DOI: 10.1124/molpharm.120.000103
This article has not been copyedited and formatted. The final version may differ from this version.

Fig. 9. Mammalian two-hybrid assays for the determination of the interaction between PGC1α and CAR or PPARα.

(A) Mammalian two-hybrid assays were performed in HepG2 cells with pGL4.31 (45 ng), the pFN11A plasmid expressing GAL4 or GAL4-PGC1α (4.5 ng), and the pFN10A plasmid expressing VP16 or VP16 fused with CAR (WT), CAR-Δ8 (Δ8) or PPARα (VP16-PPARα) (45 ng). The cells were treated with vehicle (0.2% DMSO), bezafibrate (BZF, 100 μM) and/or CITCO (1 μM) for 24 h, and the reporter activity was determined. Data are shown as the means ± S.D. (n=4). Differences in response among the GAL4-PGC1α-expressed groups were tested by one-way ANOVA. Differences vs. control VP16-expressed cells were determined by Dunnett's test (*$p < 0.05$). (B) Mammalian two-hybrid assays were performed in HepG2 cells with pGL4.31 (30 ng), the pFN11A expression plasmid for GAL4-PGC1α (3 ng), the pFN10A expression plasmid for VP16 or VP16-PPARα (30 ng), the pTargeT expression plasmid for wild-type CAR or CAR-Δ8 (3 or 30 ng). The cells were treated with vehicle (0.2% DMSO), bezafibrate (BZF, 100 μM) and/or CITCO (1 μM) for 24 h, and the reporter activity was determined. Data are shown as the means ± S. D. (n=4). Differences in response among the GAL4-PGC1α-expressed groups were tested by one-way ANOVA. Differences between the indicated combinations were determined by Bonferroni's correction (*$p < 0.05$; NS, not significant).

Fig. 10. The influence of SR18292 treatment on phenobarbital-dependent TG elevation in mouse plasma.

Mice were treated with vehicle (saline or corn oil) or phenobarbital (PB, 100 mg/kg, in saline) with or without SR18292 (45 mg/kg, in corn oil) for 24 h. (A) Plasma TG concentrations were determined with a commercial kit. Data are shown as the means ± S. D. (n=4-5). (B) qRT-PCR was performed using hepatic total RNA. The mRNA levels of the indicated target genes were normalized to those of *Actb.* Numbers shown above columns indicate the ratio to the corresponding vehicle-treated group. Data are shown as the means ± S. D. with the plots of individual mouse data (n=4-5). Differences in response among the groups

Molecular Pharmacology Fast Forward. Published on September 5, 2020 as DOI: 10.1124/molpharm.120.000103
This article has not been copyedited and formatted. The final version may differ from this version.

were tested by one-way ANOVA. Differences between the indicated combinations were determined by Bonferroni's correction (*$p < 0.05$; NS, not significant).

Molecular Pharmacology Fast Forward. Published on September 5, 2020 as DOI: 10.1124/molpharm.120.000103
This article has not been copyedited and formatted. The final version may differ from this version.

Table 1. DNA microarray and qRT-PCR analysis of the livers from TCPOBOP-treated mice.

Gene Symbol	Gene Description	Relative mRNA levels vs control	
		Microarray	qRT-PCR
Insulin signal			
Ceacam1	*CEA-related cell adhesion molecule 1*	0.4 *	0.39±0.07*
Grb7	*growth factor receptor bound protein 7*	0.5 *	0.55±0.10*
Igfbp1	*insulin-like growth factor binding protein 1*	0.1 *	0.16±0.09*
Irs2	*insulin receptor substrate 2*	0.3 *	0.21±0.06*
Pik3c3	*phosphoinositide-3-kinase, class 3*	0.5 *	0.69±0.15*
Pik3cb	*phosphatidylinositol 3-kinase, catalytic, beta polypeptide*	3.7 *	4.26±1.73*
Lipid metabolism			
Acat3	*acetyl-Coenzyme A acetyltransferase 3*	0.5 *	0.40±0.07*
Cpt1a	*carnitine palmitoyltransferase 1a, liver*	0.4 *	0.53±0.13*
Hmgcs2	*3-hydroxy-3-methylglutaryl-Coenzyme A synthase 2*	0.4 *	0.38±0.12*
Vldlr	*very low density lipoprotein receptor*	4.3	4.43±1.18*
Transcription factor			
Cebpa	*CCAAT/enhancer binding protein (C/EBP), alpha*	0.4 *	0.44±0.08*
Foxo1	*forkhead box O1*	0.5 *	0.48±0.11*
Klf15	*Kruppel-like factor 15*	0.5	0.28±0.07*
Ppara	*peroxisome proliferator activated receptor alpha*	0.3 *	0.72±0.21*
Srebf1	*sterol regulatory element binding factor 1*	0.5	0.34±0.22*

Mice were treated with TCPOBOP for 5 days. Hepatic RNA was subjected to DNA microarray and qRT-PCR analyses. The mRNA levels of the genes, in which more than 2-fold changes were observed in DNA microarray analysis, were also determined by qRT-PCR. The mRNA levels were normalized to those of *Actb* (raw Ct-values were 20 ± 0.9), and the normalized values in control (vehicle-treated) mice were set as 1 for each gene. Data are shown as the means ± S. D. (n = 3). *$p < 0.05$; **$p < 0.01$ (Student's t-test).

Figure 1

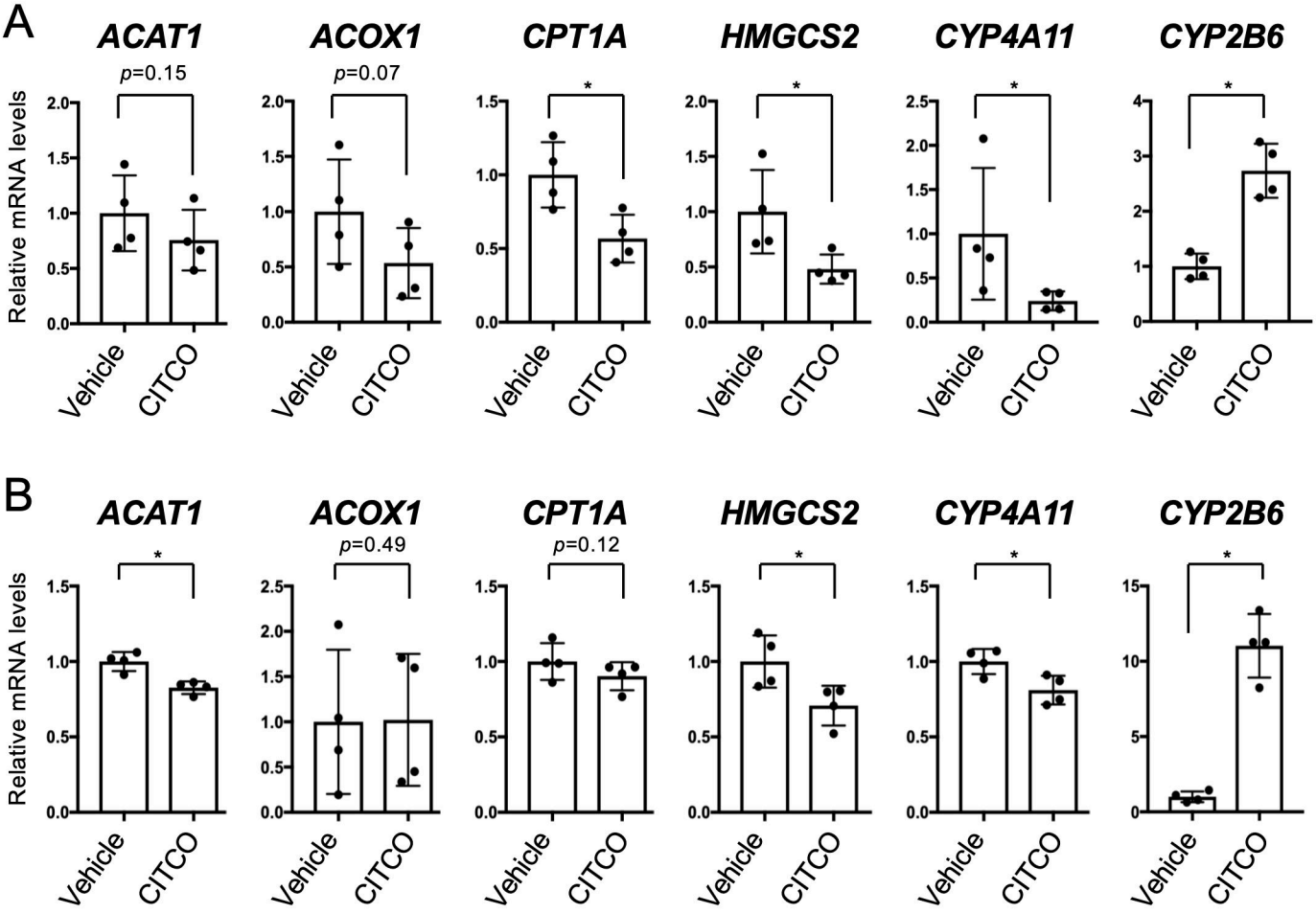
A
ACAT1
p=0.15
ACOX1
p=0.07
CPT1A
HMGCS2
CYP4A11
CYP2B6
Relative mRNA levels
Vehicle
CITCO
B
ACAT1
ACOX1
p=0.49
CPT1A
p=0.12
HMGCS2
CYP4A11
CYP2B6
Relative mRNA levels
Vehicle
CITCO

Figure 2

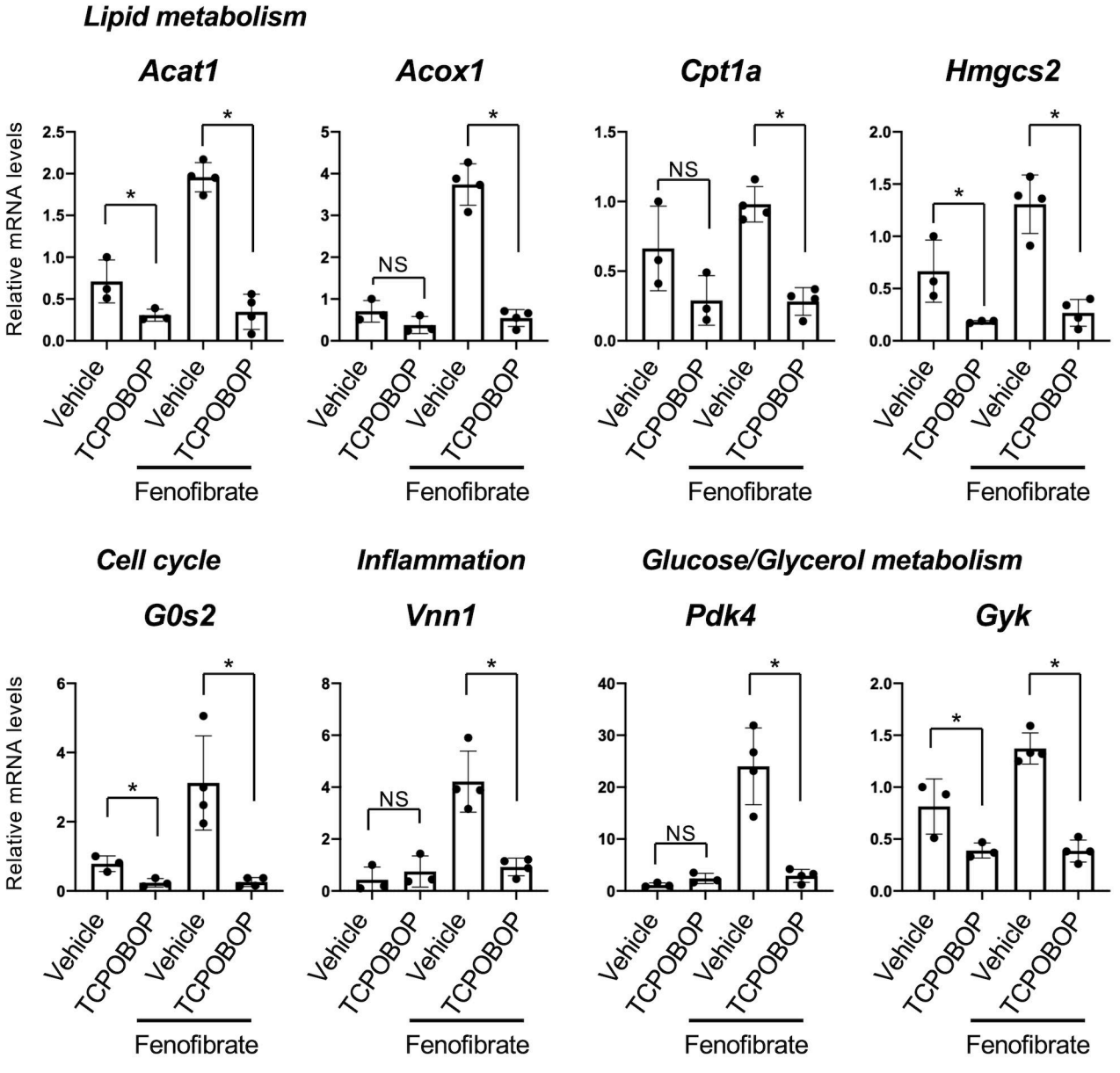
Lipid metabolism
Acat1
Acox1
Cpt1a
Hmgcs2
Relative mRNA levels
NS
*
Vehicle
TCPOBOP
Fenofibrate
Cell cycle
Inflammation
Glucose/Glycerol metabolism
G0s2
Vnn1
Pdk4
Gyk

Figure 3

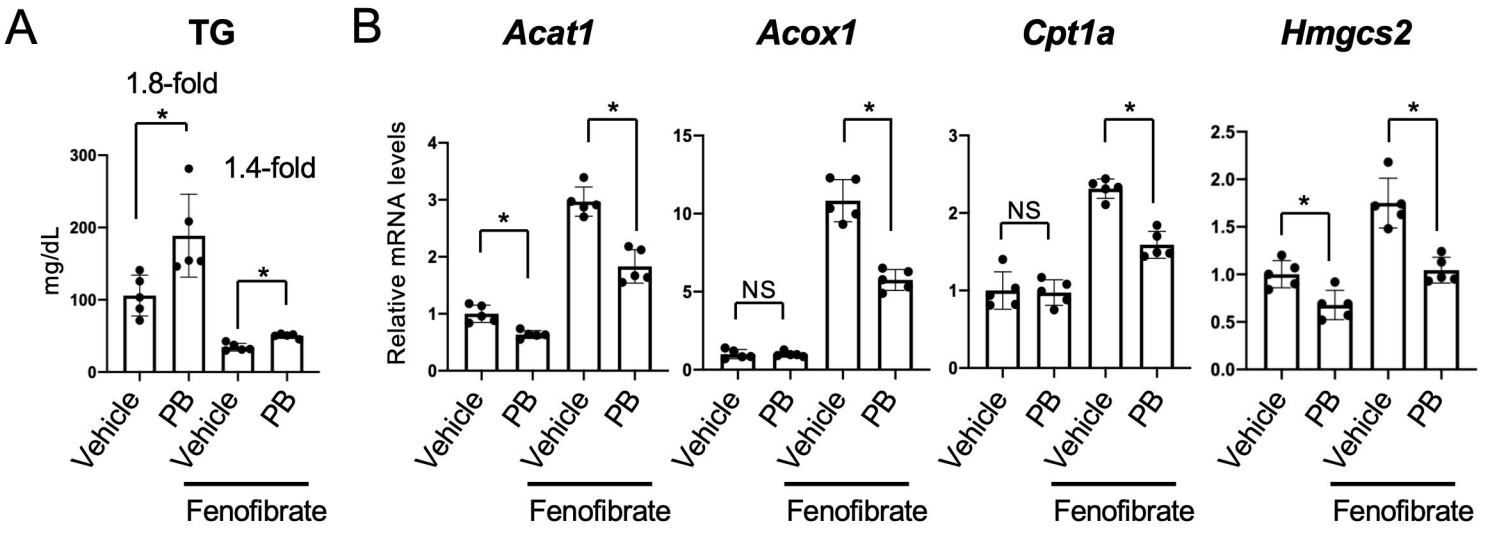
A
TG
1.8-fold
1.4-fold
mg/dL
300
200
100
0
*
*
*
Vehicle
PB
Vehicle
PB
Fenofibrate
B
Acat1
Acox1
Cpt1a
Hmgcs2
Relative mRNA levels
NS
NS
Vehicle
PB
Vehicle
PB
Fenofibrate

Figure 4

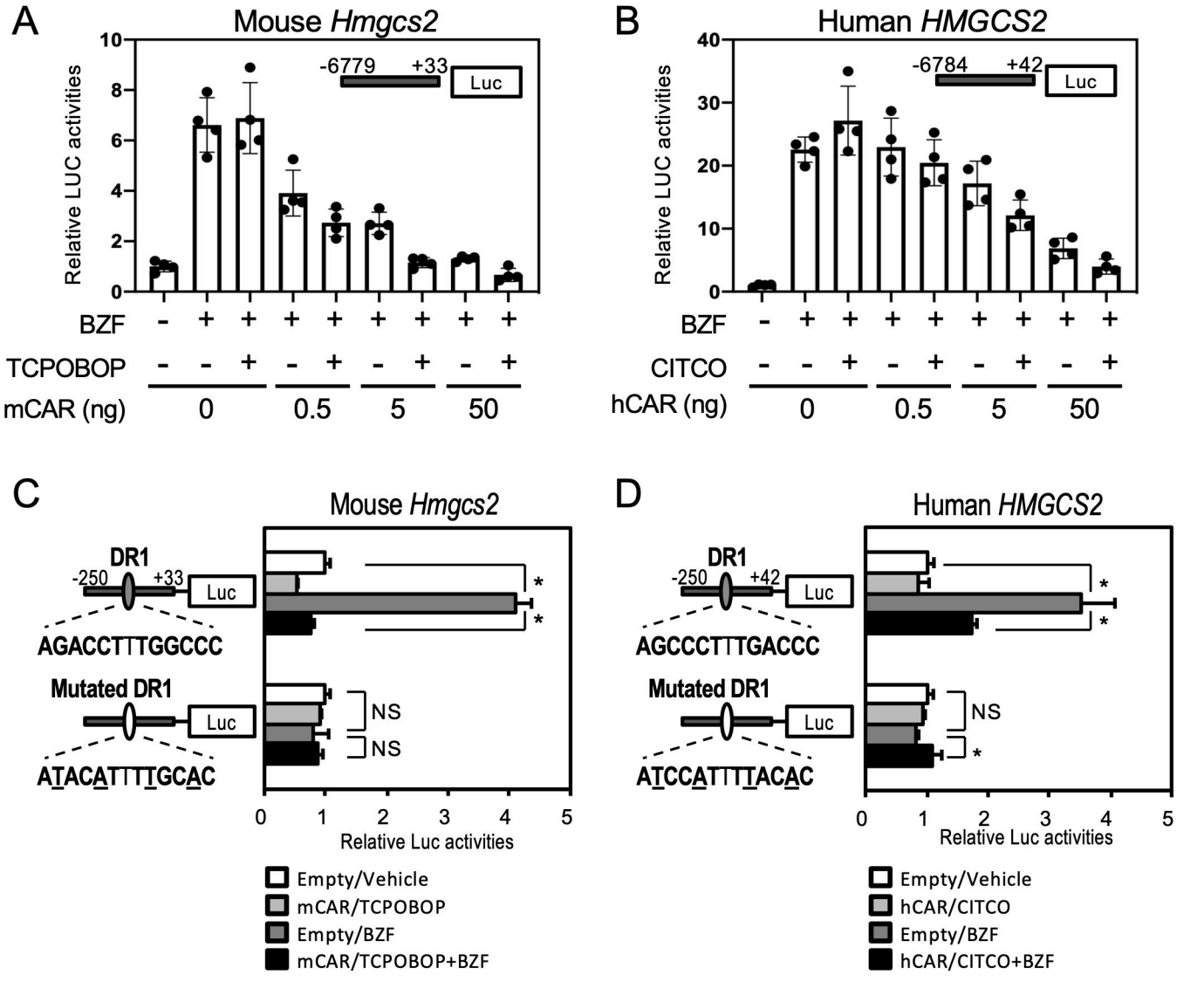
A
Mouse Hmgcs2
Relative LUC activities
-6779
+33
Luc
BZF
TCPOBOP
mCAR (ng)
0
0.5
5
50
B
Human HMGCS2
-6784
+42
CITCO
hCAR (ng)
C
Mouse Hmgcs2
DR1
-250
+33
AGACCTTTGGCCC
Mutated DR1
ATACATTTTGCAC
NS
Relative Luc activities
Empty/Vehicle
mCAR/TCPOBOP
Empty/BZF
mCAR/TCPOBOP+BZF
D
Human HMGCS2
+42
AGCCCTTTGACCC
ATCCATTTTACAC
hCAR/CITCO
hCAR/CITCO+BZF

Figure 5

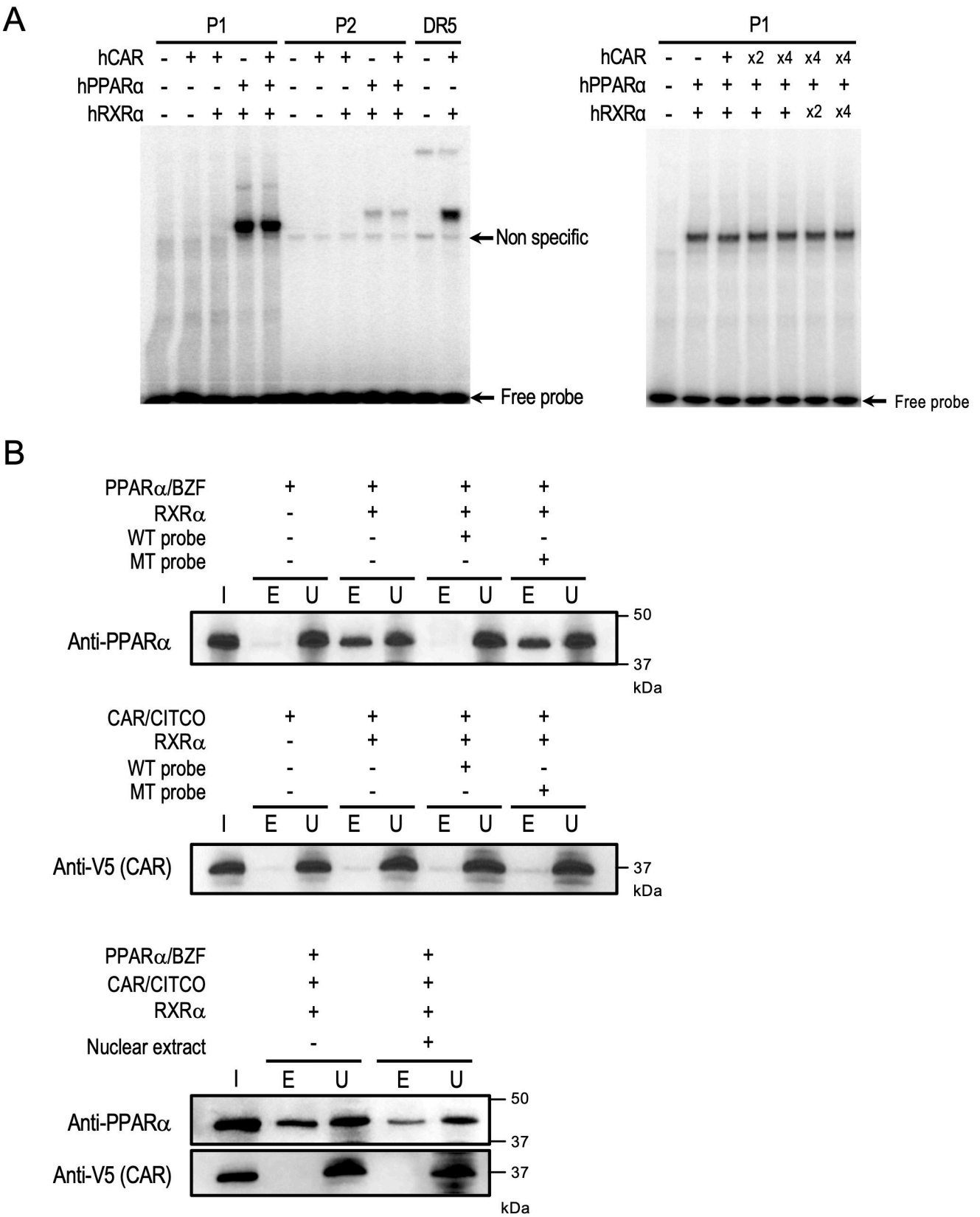
A
P1
P2
DR5
hCAR - + + - + - + + - + - +
hPPARα - - - + + - - - + + - -
hRXRα - - + + + - - + + + - +
Non specific
Free probe
P1
hCAR - - + x2 x4 x4 x4
hPPARα - + + + + + +
hRXRα - + + + + x2 x4
Free probe
B
PPARα/BZF + + + +
RXRα - + + +
WT probe - - + -
MT probe - - - +
I E U E U E U E U
Anti-PPARα
50
37
kDa
CAR/CITCO + + + +
RXRα - + + +
WT probe - - + -
MT probe - - - +
I E U E U E U E U
Anti-V5 (CAR)
37
kDa
PPARα/BZF + +
CAR/CITCO + +
RXRα + +
Nuclear extract - +
I E U E U
Anti-PPARα
50
37
Anti-V5 (CAR)
37
kDa

Figure 6

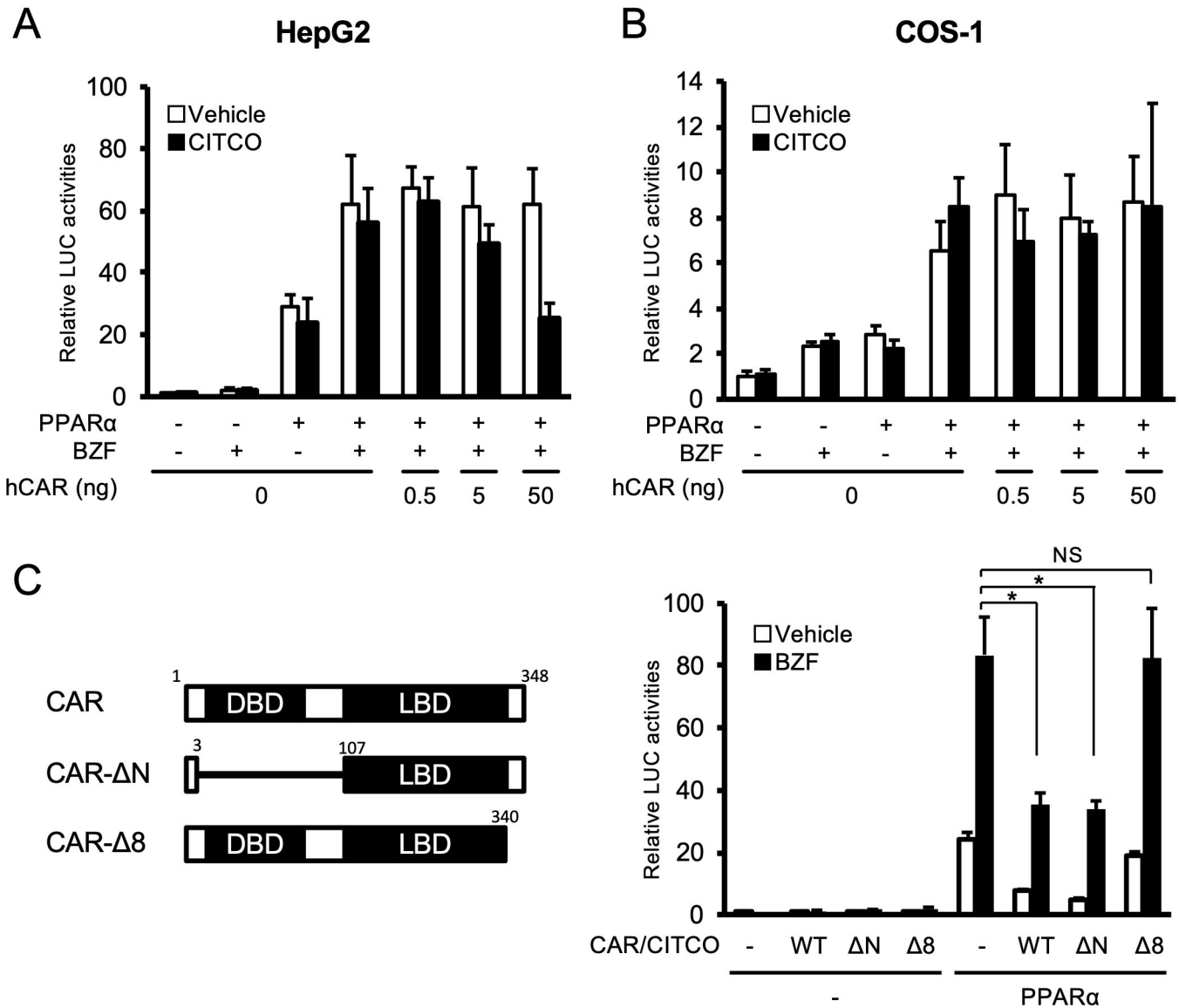
A
HepG2
Relative LUC activities
Vehicle
CITCO
PPARα
BZF
hCAR (ng)
B
COS-1
C
CAR
CAR-ΔN
CAR-Δ8
DBD
LBD
1
348
3
107
340
NS
*
Vehicle
BZF
CAR/CITCO
WT
ΔN
Δ8
PPARα

Figure 7

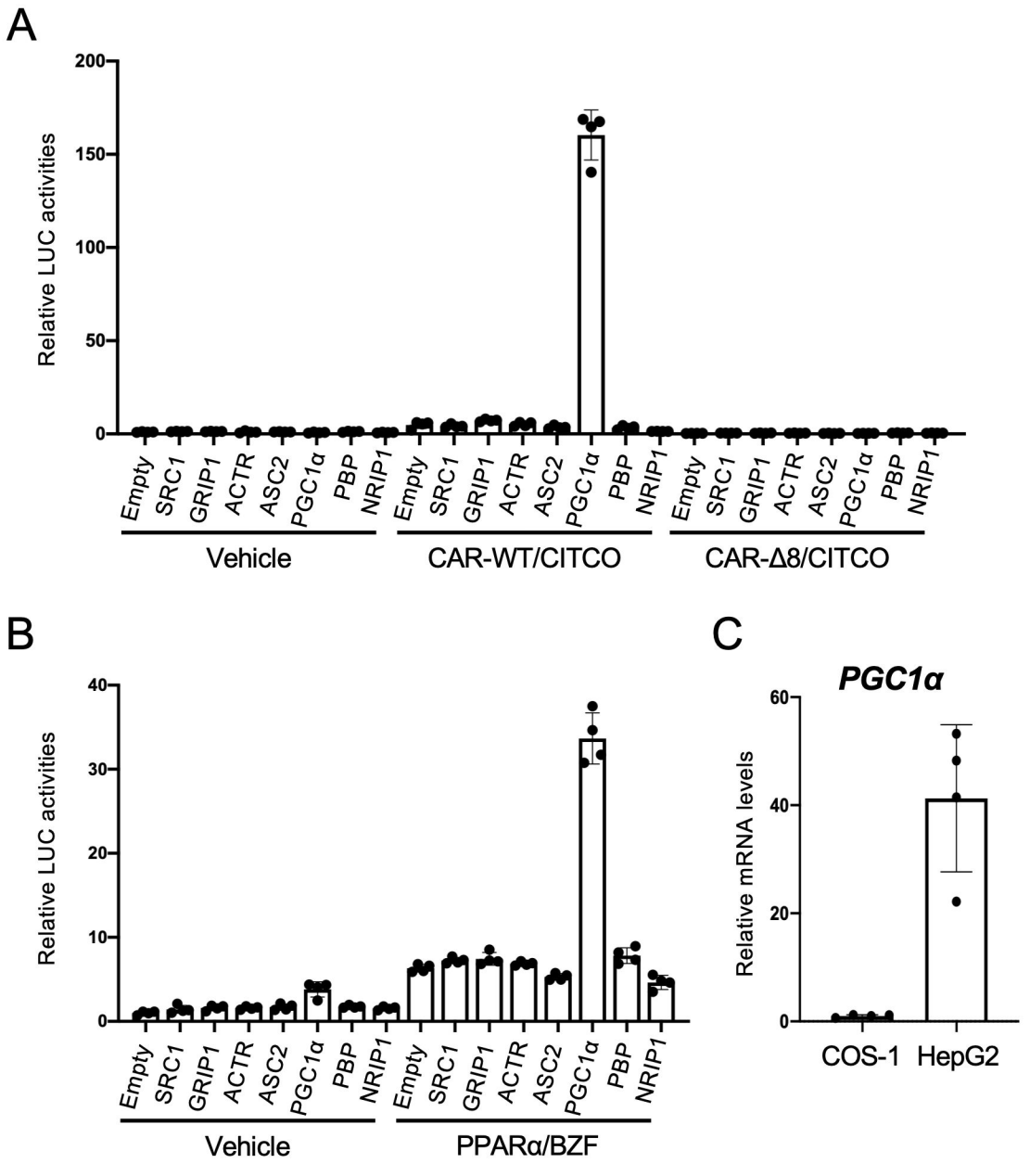
A
Relative LUC activities
200
150
100
50
0
Empty
SRC1
GRIP1
ACTR
ASC2
PGC1α
PBP
NRIP1
Vehicle
CAR-WT/CITCO
CAR-Δ8/CITCO
B
Relative LUC activities
40
30
20
10
0
PPARα/BZF
C
PGC1α
Relative mRNA levels
60
40
20
0
COS-1
HepG2

Figure 8

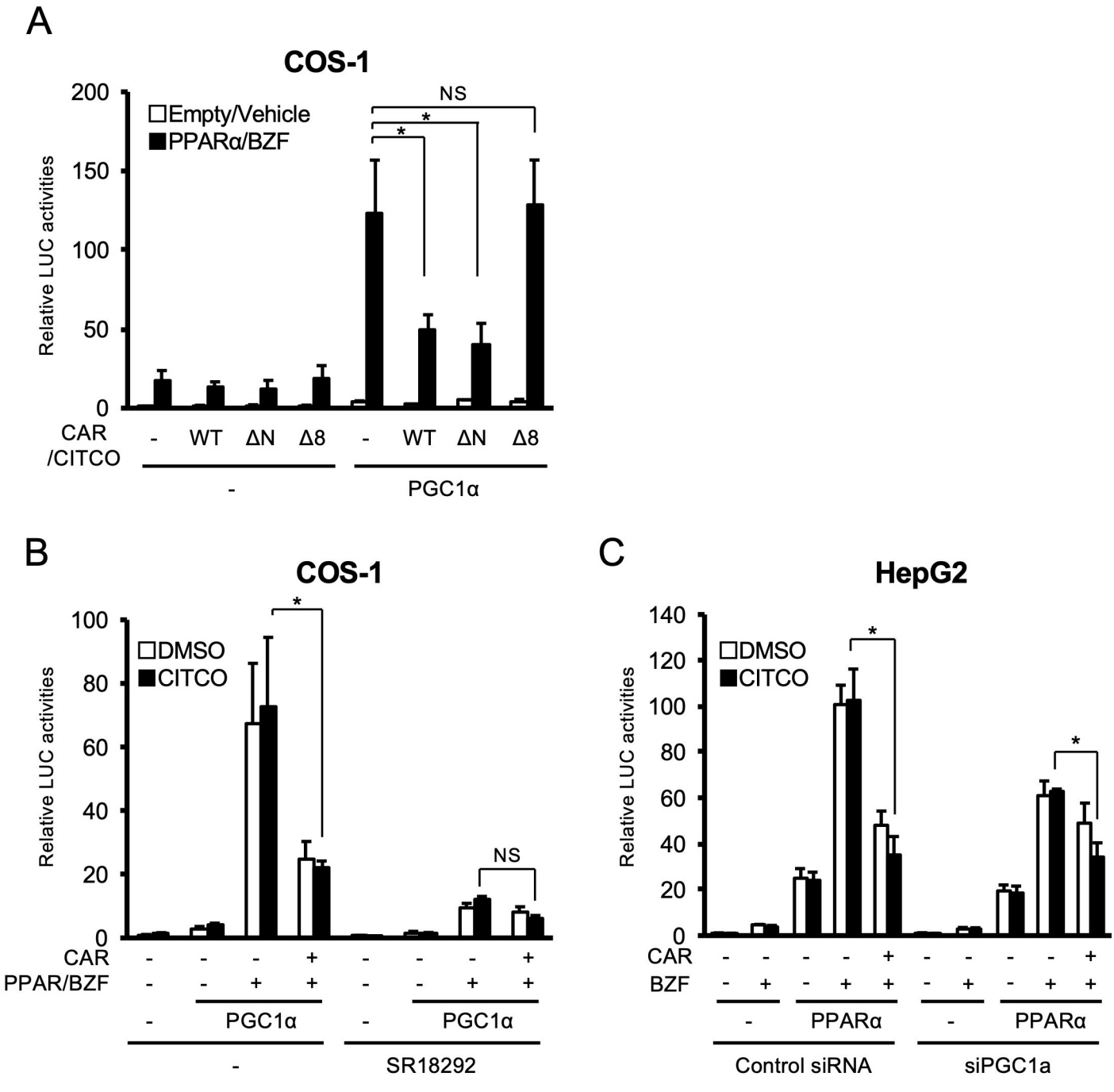
A
COS-1
Relative LUC activities
200
150
100
50
0
□Empty/Vehicle
■PPARα/BZF
NS
*
*
CAR /CITCO
-
WT
ΔN
Δ8
-
WT
ΔN
Δ8
-
PGC1α
B
COS-1
Relative LUC activities
100
80
60
40
20
0
□DMSO
■CITCO
*
NS
CAR
PPAR/BZF
PGC1α
PGC1α
-
SR18292
C
HepG2
Relative LUC activities
140
120
100
80
60
40
20
0
□DMSO
■CITCO
*
*
CAR
BZF
PPARα
PPARα
Control siRNA
siPGC1a

Figure 9

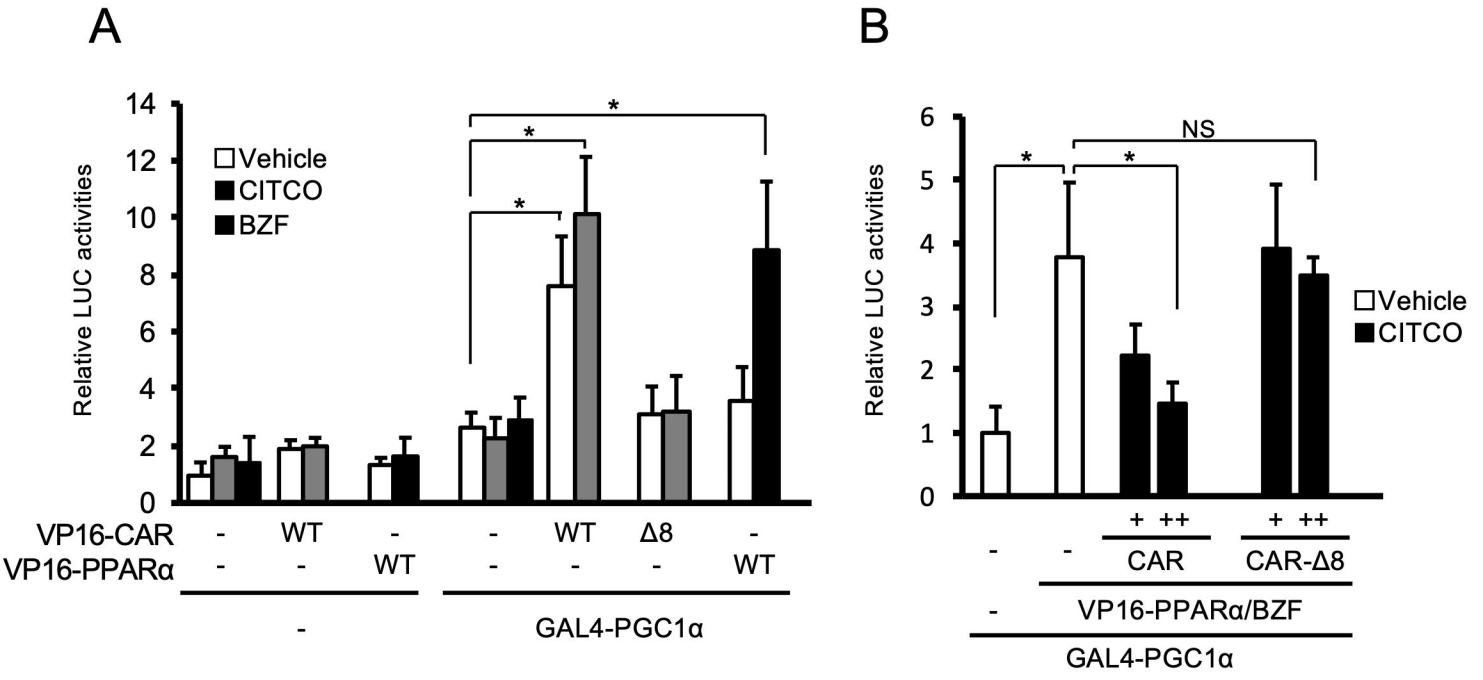
A
Relative LUC activities
14
12
10
8
6
4
2
0
Vehicle
CITCO
BZF
*
*
*
VP16-CAR - WT - - WT Δ8 -
VP16-PPARα - - WT - - - WT
- GAL4-PGC1α
B
Relative LUC activities
6
5
4
3
2
1
0
NS
*
*
Vehicle
CITCO
+ ++ + ++
- - CAR CAR-Δ8
- VP16-PPARα/BZF
GAL4-PGC1α

Figure 10

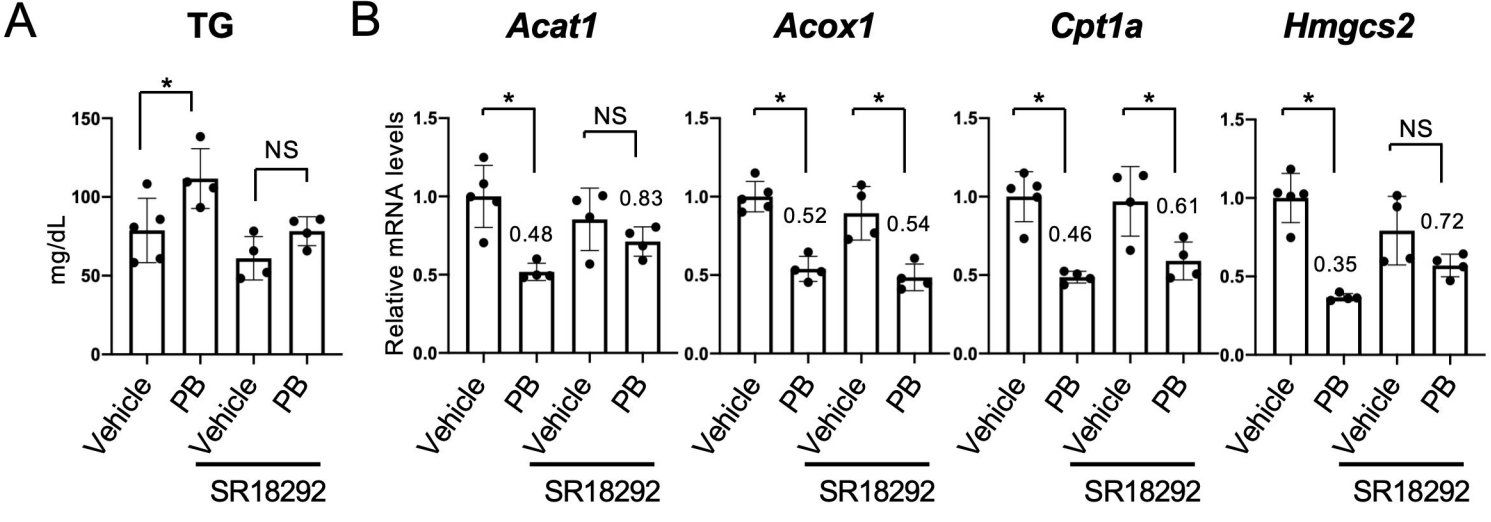
A
TG
mg/dL
150
100
50
0
*
NS
Vehicle
PB
Vehicle
PB
SR18292
B
Acat1
Acox1
Cpt1a
Hmgcs2
Relative mRNA levels
1.5
1.0
0.5
0.0
*
NS
0.48
0.83
0.52
0.54
0.46
0.61
0.35
0.72
Vehicle
PB
Vehicle
PB
SR18292

Supplemental Data

Antiepileptic drug-activated constitutive androstane receptor inhibits peroxisome proliferator-activated receptor α- and peroxisome proliferator-activated receptor γ coactivator 1α-dependent gene expression to increase blood triglyceride levels

Ryota Shizu[1], Yuta Otsuka[2], Kanako Ezaki[1], Chizuru Ishii[2], Shingo Arakawa[3], Yuto Amaike[1], Taiki Abe[1,2], Takuomi Hosaka[1], Takamitsu Sasaki[1], Yuichiro Kanno[1], Masaaki Miyata[2], Yasushi Yamazoe[2], Kouichi Yoshinari[1,2]

[1]Laboratory of Molecular Toxicology, School of Pharmaceutical Sciences, University of Shizuoka, 52-1 Yada, Suruga-ku, Shizuoka 422-8526 Japan

[2]Graduate School of Pharmaceutical Sciences, Tohoku University, 6-3 Aramaki-aoba, Aoba-ku, Sendai, Miyagi 980-8578, Japan

[3]Pharmacovigilance Department, Clinical Safety & Pharmacovigilance Division, Daiichi Sankyo Co., Ltd., 3-5-1, Nihonbashi-honcho, Chuo-ku, Tokyo 103-8426 Japan

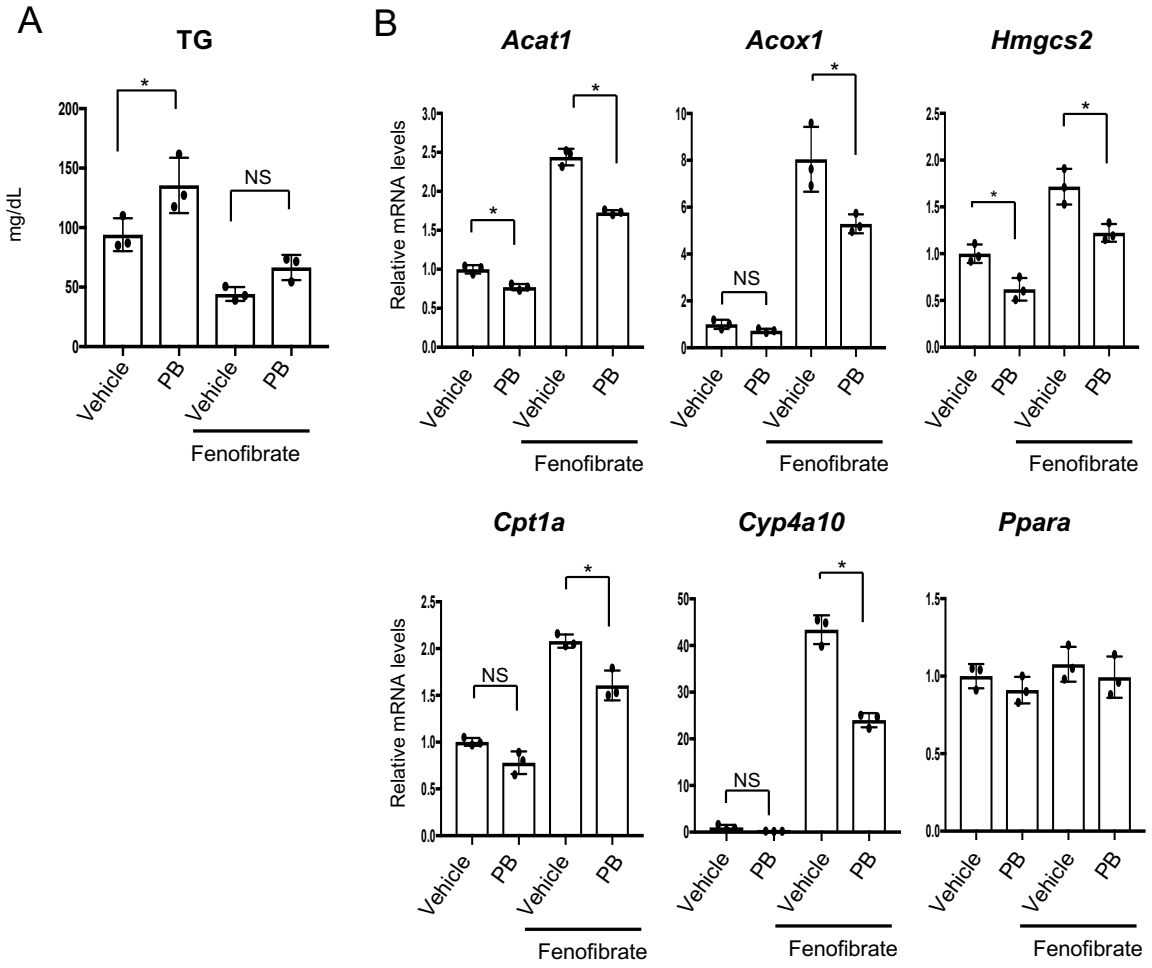

Fig. S1. Influence of phenobarbital treatment on the expression levels of PPARα target genes in the liver of fenofibrate-treated mice.

Mice were treated with 300 ppm fenofibrate and/or 300 ppm phenobarbital (PB) for a week. (A) Plasma TG concentrations were determined using a commercial kit. (B) mRNA levels of PPARα target genes were determined by qRT-PCR. Data are shown as the mean ± S. D. with the plots of individual mouse data (n = 3). Statistical analyses were performed for the indicated combinations with Bonferroni's correction (*$p < 0.05$; NS, not significant).

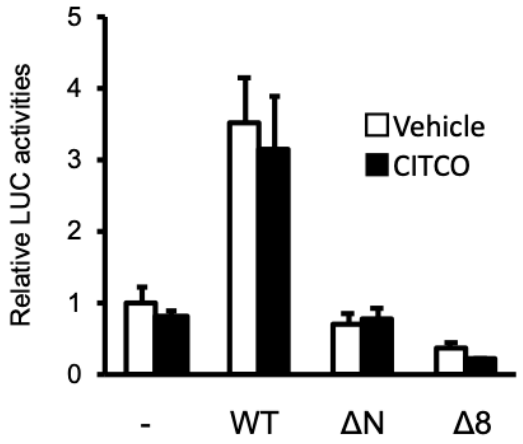

Fig. S2. The transcriptional activity of CAR mutants.

Reporter gene assays were performed in COS-1 cells with $(NR1)_5$-tk-pGL3, expression plasmids for CAR-WT, CAR-ΔN or CAR-Δ8, and phRL-SV40. The cells were treated with vehicle (0.1% DMSO) or CITCO (1 μM) and reporter activity was determined. Data are shown as the mean ± S. D. (n = 4).

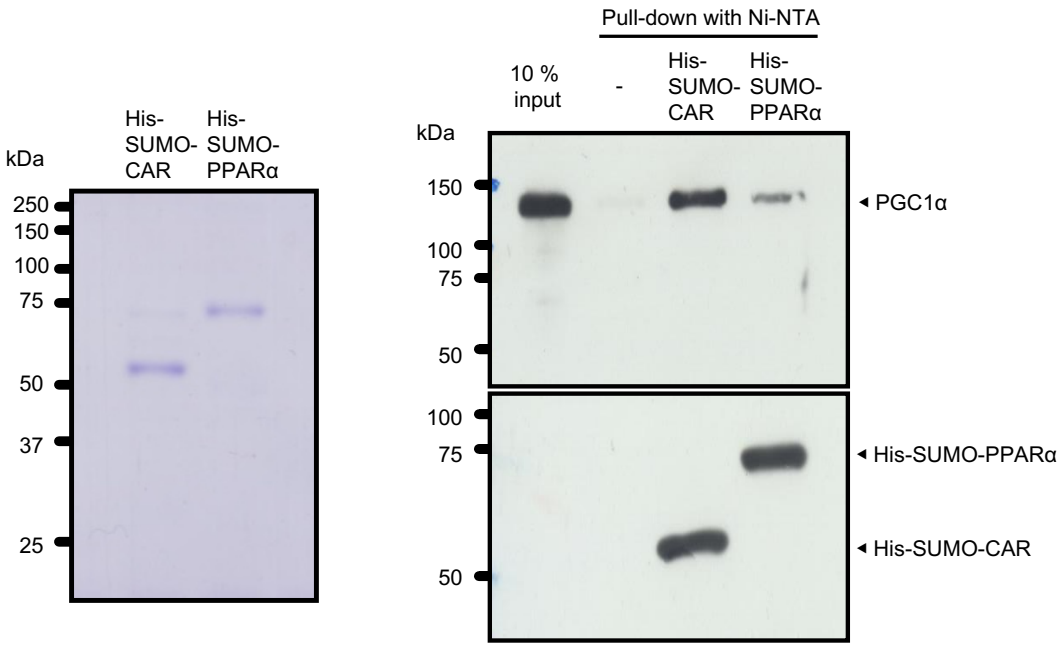

Fig. S3. **The binding of PGC1α with CAR or PPARα**

Pull-down assays were performed with recombinant His-SUMO-CAR or His-SUMO-PPARα, which were purified as described in *Experimental Procedures,* and *in vitro* synthesized PGC1α. The reaction mixture was then incubated with Ni-NTA and the amount of PGC1α precipitated was determined by immunoblotting with anti-PGC1α antibody. Anti-His antibody was used to confirm the amount of His-SUMO-CAR and His-SUMO-PPARα.

Table S1. Microarray analysis of the liver from TCPOBOP-treated mice.

Gene Symbol	Gene Description	Vehicle					TCPOBOP					TCPOBOP /Vehicle	p-value
		1	2	3	Average	C.V.	1	2	3	Average	C.V.		
Abca1	ATP-binding cassette, sub-family A (ABC1), member 1	502.327	306.782	393.530	400.880	24.441	225.400	176.261	398.119	266.593	43.709	0.665	0.101
Abcc8	ATP-binding cassette, sub-family C (CFTR/MRP), member 8	21.077	26.572	20.604	22.751	14.582	7.513	7.541	12.004	9.019	28.657	ND	ND
Acaa1a	acetyl-Coenzyme A acyltransferase 1A	1419.162	1031.463	756.155	1068.927	31.161	537.203	590.051	826.248	651.167	23.636	0.609	0.060
Acaca	acetyl-Coenzyme A carboxylase alpha	154.562	258.470	278.150	230.394	28.822	355.005	190.400	120.036	221.813	54.367	0.963	0.460
Acadm	acyl-Coenzyme A dehydrogenase, medium chain	3031.527	1524.247	1497.888	2017.887	43.508	1094.128	1177.275	2176.653	1482.685	40.631	0.735	0.217
Acads	acyl-Coenzyme A dehydrogenase, short chain	590.147	541.095	471.824	534.356	11.125	307.107	401.536	384.115	364.253	13.795	0.682	0.010
Acat1	acetyl-Coenzyme A acetyltransferase 1	3670.853	1529.078	1574.122	2258.017	54.196	749.454	967.081	1738.522	1151.685	45.128	0.510	0.111
Acat2	acetyl-Coenzyme A acetyltransferase 2	1348.907	1444.532	1244.463	1345.967	7.435	755.089	959.540	964.289	892.973	13.375	0.663	0.004
Acat3	acetyl-Coenzyme A acetyltransferase 3	2406.253	2645.087	2548.676	2533.339	4.743	1070.649	1298.867	1302.391	1223.969	10.849	0.483	0.000
Ace	angiotensin I converting enzyme (peptidyl-dipeptidase A) 1	10.538	16.909	8.241	11.896	37.748	3.757	4.713	8.002	5.491	40.563	ND	ND
Acly	ATP citrate lyase	1391.060	1176.400	1456.681	1341.380	10.929	1387.148	755.944	662.199	935.097	42.165	0.697	0.085
Acox1	acyl-Coenzyme A oxidase 1, palmitoyl	7120.400	4959.237	6554.033	6211.223	18.042	2661.595	3583.665	2616.785	2954.015	18.475	0.476	0.005
Acox2	acyl-Coenzyme A oxidase 2, branched chain	1331.343	1268.193	1170.289	1256.608	6.458	1024.630	1283.785	1084.325	1130.913	12.000	0.900	0.120
Acsl1	acyl-CoA synthetase long-chain family member 1	9688.241	5766.049	4528.691	6660.993	40.440	3948.252	4869.336	5903.771	4907.120	19.936	0.737	0.174
Acsl4	acyl-CoA synthetase long-chain family member 4	453.148	130.443	140.105	241.232	76.105	179.381	92.372	528.158	266.637	86.494	1.105	0.444
Acsl5	acyl-CoA synthetase long-chain family member 5	5616.932	2978.441	3475.842	4023.738	34.843	2015.449	1653.274	4287.286	2652.003	53.836	0.659	0.150
Acss2	acyl-CoA synthetase short-chain family member 2	1601.827	1775.470	1477.284	1618.194	9.255	699.678	656.974	606.182	654.278	7.154	0.404	0.000

Adipoq	adiponectin, C1Q and collagen domain containing	14.051	16.909	10.302	13.754	24.092	5.635	6.598	10.003	7.412	30.963	ND	ND
Adipor1	adiponectin receptor 1	1004.654	698.110	1054.909	919.224	21.010	766.359	971.793	834.250	857.468	12.206	0.933	0.326
Adipor2	adiponectin receptor 2	2040.924	1613.624	1858.453	1837.667	11.667	756.967	669.227	708.212	711.469	6.179	0.387	0.000
Adra1a	adrenergic receptor, alpha 1a	14.051	12.078	16.483	14.204	15.534	4.696	10.368	8.002	7.689	37.056	ND	ND
Adra1b	adrenergic receptor, alpha 1b	249.407	565.252	690.224	501.627	45.291	423.564	558.946	216.065	399.525	43.226	0.796	0.285
Adra1d	adrenergic receptor, alpha 1d	10.538	4.831	8.241	7.870	36.486	2.817	2.828	8.002	4.549	65.738	ND	ND
Adra2a	adrenergic receptor, alpha 2a	14.051	7.247	8.241	9.846	37.324	3.757	3.770	10.003	5.843	61.650	ND	ND
Adra2b	adrenergic receptor, alpha 2b	35.128	41.065	22.664	32.952	28.500	15.966	12.253	12.004	13.408	16.550	ND	ND
Adra2c	adrenergic receptor, alpha 2c	21.077	62.806	41.207	41.697	50.049	26.297	31.105	10.003	22.468	49.224	ND	ND
Adrb3	adrenergic receptor, beta 3	45.666	16.909	20.604	27.726	56.429	14.087	5.655	8.002	9.248	47.056	ND	ND
Agt	angiotensinogen (serpin peptidase inhibitor, clade A, member 8)	3979.977	6022.103	5404.347	5135.476	20.393	2429.621	3362.160	2560.768	2784.183	18.132	0.542	0.012
Agtr1b	angiotensin II receptor, type 1b	706.068	352.678	403.832	487.526	39.174	130.544	159.295	298.089	195.976	45.717	0.402	0.037
Agtr2	angiotensin II receptor, type 2	10.538	4.831	4.121	6.497	54.151	3.757	1.885	6.002	3.881	53.106	ND	ND
Agtrl1	angiotensin receptor-like 1	10.538	12.078	18.543	13.720	30.959	3.757	16.966	12.004	10.909	61.166	ND	ND
Akt1	thymoma viral proto-oncogene 1	165.101	335.769	206.037	235.636	37.813	185.955	254.495	160.048	200.166	24.380	0.849	0.289
Akt2	thymoma viral proto-oncogene 2	295.073	471.043	331.719	365.945	25.371	291.141	434.526	242.073	322.580	31.001	0.881	0.306
Akt3	thymoma viral proto-oncogene 3	17.564	16.909	18.543	17.672	4.654	6.574	20.737	20.006	15.772	50.558	ND	ND
Angptl4	angiopoietin-like 4	871.169	859.955	881.838	870.987	1.256	141.814	279.944	206.062	209.273	33.029	0.240	0.000
Angptl6	angiopoietin-like 6	108.896	101.455	74.173	94.842	19.276	55.411	76.348	70.021	67.260	15.966	ND	ND
Apoa1	apolipoprotein A-I	64501.625	45256.356	37587.308	49115.096	28.231	25535.911	40640.008	46093.828	37423.249	28.458	0.762	0.156
Apoa2	apolipoprotein A-II	97953.807	77521.589	67631.606	81035.667	19.082	41808.833	61360.605	65639.692	56269.710	22.579	0.694	0.049
Apoc3	apolipoprotein C-III	33339.773	26202.065	26714.742	28752.194	13.847	20378.953	27905.837	24029.209	24104.666	15.615	0.838	0.108

Apod	apolipoprotein D	158.075	60.390	76.234	98.233	53.370	34.749	30.162	26.008	30.306	14.427	ND	ND
Apoe	apolipoprotein E	83670.853	48014.977	54956.217	62214.016	30.385	18775.798	22976.176	36212.864	25988.279	35.017	0.418	0.020
Ar	androgen receptor	21.077	9.662	14.423	15.054	38.085	12.209	6.598	20.006	12.938	52.046	ND	ND
Araf	v-raf murine sarcoma 3611 viral oncogene homolog	221.305	369.588	271.969	287.620	26.205	238.548	304.451	230.069	257.689	15.801	0.896	0.289
B2m	beta-2 microglobulin	25548.432	27907.482	29242.814	27566.243	6.786	13881.806	18230.318	22290.687	18134.270	23.190	0.658	0.012
Bcl2l1	Bcl2-like 1	154.562	217.404	162.769	178.245	19.165	88.282	123.477	74.022	95.260	26.722	0.534	0.014
C3	complement component 3	37105.471	62052.056	50106.109	49754.545	25.077	34054.143	54102.788	43651.095	43936.009	22.823	0.883	0.282
Camkk1	calcium/calmodulin-dependent protein kinase kinase 1, alpha	7.026	4.831	6.181	6.013	18.408	2.817	2.828	6.002	3.882	47.279	ND	ND
Camkk2	calcium/calmodulin-dependent protein kinase kinase 2, beta	35.128	50.728	51.509	45.788	20.181	22.540	26.392	26.008	24.980	8.494	ND	ND
Cap1	CAP, adenylate cyclase-associated protein 1 (yeast)	165.101	67.637	74.173	102.304	53.255	30.992	39.588	34.010	34.864	12.508	0.341	0.050
Ccl2	chemokine (C-C motif) ligand 2	52.692	115.949	65.932	78.191	42.669	45.080	50.899	68.020	54.666	21.815	ND	ND
Ccl5	chemokine (C-C motif) ligand 5	28.102	33.818	37.087	33.002	13.779	20.662	29.220	32.010	27.297	21.663	ND	ND
Ccnd1	cyclin D1	73.768	161.846	117.441	117.685	37.421	298.655	446.780	274.082	339.839	27.491	2.888	0.010
Ccr2	chemokine (C-C motif) receptor 2	14.051	26.572	20.604	20.409	30.685	8.452	7.541	22.007	12.667	63.960	ND	ND
Cd28	CD28 antigen	10.538	7.247	8.241	8.676	19.459	2.817	3.770	10.003	5.530	70.570	ND	ND
Cd36	CD36 antigen	730.658	601.486	486.247	606.130	20.172	202.860	206.424	720.216	376.500	79.063	0.621	0.142
Cdkn1a	cyclin-dependent kinase inhibitor 1A (P21)	147.537	84.546	150.407	127.497	29.196	154.023	134.788	152.046	146.952	7.200	1.153	0.217
Ceacam1	CEA-related cell adhesion molecule 1	821.990	548.342	568.662	646.331	23.589	175.624	248.839	430.129	284.864	45.994	0.441	0.018
Cebpa	CCAAT/enhancer binding protein (C/EBP), alpha	874.682	555.589	541.877	657.383	28.646	233.852	245.069	370.111	283.011	26.727	0.431	0.017
Cebpb	CCAAT/enhancer binding protein (C/EBP), beta	1605.339	2444.592	3702.483	2584.138	40.846	1218.098	1994.486	1162.349	1458.311	31.898	0.564	0.083
Cebpd	CCAAT/enhancer binding protein (C/EBP), delta	17.564	9.662	14.423	13.883	28.656	9.392	10.368	10.003	9.921	4.974	ND	ND
Cfb	complement factor B	11469.219	20269.340	17848.975	16529.178	27.503	6774.201	9789.570	6587.976	7717.249	23.287	0.467	0.018

Cfd	complement factor D (adipsin)	10.538	48.312	6.181	21.677	106.883	3.757	1.885	8.002	4.548	68.919	ND	ND
Cfh	complement component factor h	11578.115	9983.695	13441.846	11667.885	14.834	2197.647	1955.840	8782.635	4312.041	89.831	0.370	0.020
Cfi	complement component factor i	7865.109	6111.480	7444.112	7140.234	12.821	2198.587	2954.969	6113.834	3755.796	55.297	0.526	0.031
Clu	clusterin	10612.102	18737.846	17047.492	15465.813	27.723	21035.430	27127.271	25497.649	24553.450	12.845	1.588	0.021
Cpt1a	carnitine palmitoyltransferase 1a, liver	997.629	1118.425	972.494	1029.516	7.578	346.552	405.307	414.124	388.661	9.451	0.378	0.000
Creb1	cAMP responsive element binding protein 1	77.281	38.650	43.268	53.066	39.757	21.601	19.794	38.011	26.469	37.920	ND	ND
Crebbp	CREB binding protein	56.204	57.975	37.087	50.422	22.971	35.688	38.646	40.012	38.115	5.798	ND	ND
Crk	v-crk sarcoma virus CT10 oncogene homolog (avian)	484.763	338.185	344.082	389.010	21.330	164.354	164.008	256.077	194.813	27.235	0.501	0.013
Crp	C-reactive protein, pentraxin-related	3056.117	2060.511	3214.175	2776.934	22.523	1598.460	2754.200	3931.179	2761.280	42.240	0.994	0.492
Csf1	colony stimulating factor 1 (macrophage)	42.153	62.806	61.811	55.590	20.952	49.776	66.923	42.013	52.904	24.093	ND	ND
Ctla4	cytotoxic T-lymphocyte-associated protein 4	14.051	4.831	4.121	7.668	72.246	3.757	2.828	8.002	4.862	56.739	ND	ND
Ctnnb1	catenin (cadherin associated protein), beta 1	839.554	1084.607	918.924	947.695	13.193	623.606	650.376	624.187	632.723	2.417	0.668	0.006
Cyp19a1	cytochrome P450, family 19, subfamily a, polypeptide 1	10.538	4.831	6.181	7.184	41.521	2.817	1.885	6.002	3.568	60.495	ND	ND
Cyp7a1	cytochrome P450, family 7, subfamily a, polypeptide 1	217.792	388.912	335.840	314.182	27.879	410.415	626.812	2506.752	1181.326	97.597	3.760	0.132
Cyp8b1	cytochrome P450, family 8, subfamily b, polypeptide 1	1745.851	835.799	432.677	1004.776	66.950	216.947	354.408	796.239	455.865	66.397	0.454	0.133
Dcn	decorin	1830.157	1468.688	1602.967	1633.937	11.182	551.290	577.798	1768.531	965.873	71.981	0.591	0.091
Dlat	dihydrolipoamide S-acetyltransferase (E2 component of pyruvate dehydrogenase complex)	730.658	509.693	496.549	578.966	22.719	381.301	349.695	734.220	488.405	43.707	0.844	0.283
Dld	dihydrolipoamide dehydrogenase	1345.394	591.823	655.197	864.138	48.370	399.145	371.374	1522.457	764.325	85.920	0.884	0.418
Dlk1	delta-like 1 homolog (Drosophila)	14.051	4.831	8.241	9.041	51.560	3.757	1.885	12.004	5.882	91.529	ND	ND
Dpt	dermatopontin	38.641	120.780	74.173	77.865	52.905	15.027	17.909	30.009	20.982	37.889	ND	ND
Dusp1	dual specificity phosphatase 1	84.307	128.027	111.260	107.865	20.449	281.750	155.525	108.032	181.769	49.394	1.685	0.119

Dusp4	dual specificity phosphatase 4	21.077	31.403	22.664	25.048	22.200	30.992	25.449	20.006	25.483	21.557	ND	ND
Dvl1	dishevelled, dsh homolog 1 (Drosophila)	91.332	178.755	111.260	127.116	36.044	120.213	175.319	106.032	133.855	27.345	1.053	0.426
Dvl2	dishevelled 2, dsh homolog (Drosophila)	765.786	630.473	498.609	631.623	21.151	361.579	527.841	540.162	476.527	20.930	0.754	0.091
Dvl3	dishevelled 3, dsh homolog (Drosophila)	45.666	57.975	32.966	45.536	27.462	23.479	34.875	28.008	28.788	19.932	ND	ND
E2f4	E2F transcription factor 4	105.383	183.586	191.614	160.195	29.737	119.274	152.697	100.030	124.000	21.492	0.774	0.157
E2f5	E2F transcription factor 5	63.230	45.896	59.751	56.292	16.289	35.688	34.875	104.031	58.198	68.206	ND	ND
Ehhadh	enoyl-Coenzyme A, hydratase/3-hydroxyacyl Coenzyme A dehydrogenase	1735.312	1517.000	1009.581	1420.631	26.209	629.241	817.211	646.194	697.549	14.906	0.491	0.016
Eif2b1	eukaryotic translation initiation factor 2B, subunit 1 (alpha)	182.664	198.080	218.399	199.714	8.974	176.563	198.883	232.070	202.505	13.792	1.014	0.446
Eif4ebp1	eukaryotic translation initiation factor 4E binding protein 1	305.612	282.626	267.848	285.362	6.669	173.746	203.596	268.080	215.141	22.411	0.754	0.039
Enpp1	ectonucleotide pyrophosphatase/phosphodiesterase 1	189.690	132.858	125.682	149.410	23.470	60.107	65.038	140.042	88.395	50.676	0.592	0.068
Erc2	ELKS/RAB6-interacting/CAST family member 2	14.051	9.662	10.302	11.338	20.910	11.270	9.426	22.007	14.234	47.731	ND	ND
Esr1	estrogen receptor 1 (alpha)	42.153	101.455	90.656	78.088	40.449	39.445	49.956	42.013	43.805	12.510	ND	ND
Esr2	estrogen receptor 2 (beta)	17.564	9.662	6.181	11.136	52.378	6.574	2.828	8.002	5.801	46.066	ND	ND
Fabp1	fatty acid binding protein 1, liver	42919.118	24286.491	19538.477	28914.695	42.741	18128.713	15267.809	28358.508	20585.010	33.434	0.712	0.183
Fabp2	fatty acid binding protein 2, intestinal	793.888	326.107	288.452	469.482	59.975	204.738	127.247	694.208	342.065	89.871	0.729	0.312
Fabp3	fatty acid binding protein 3, muscle and heart	10.538	9.662	6.181	8.794	26.209	4.696	4.713	10.003	6.471	47.279	ND	ND
Fabp4	fatty acid binding protein 4, adipocyte	235.356	328.522	179.252	247.710	30.438	202.860	243.184	424.127	290.057	40.628	1.171	0.314
Fabp5	fatty acid binding protein 5, epidermal	533.942	543.511	1240.342	772.598	52.434	167.171	151.754	166.050	161.659	5.317	0.209	0.030
Fabp7	fatty acid binding protein 7, brain	73.768	41.065	67.992	60.942	28.641	29.114	34.875	118.035	60.675	82.009	ND	ND
Fabp9	fatty acid binding protein 9, testis	10.538	4.831	6.181	7.184	41.521	3.757	2.828	8.002	4.862	56.739	ND	ND
Fasn	fatty acid synthase	453.148	683.616	776.759	637.841	26.118	1705.525	719.184	824.247	1082.985	50.018	1.698	0.123
Fbp1	fructose bisphosphatase 1	9062.967	8940.153	9630.164	9211.095	3.996	3308.680	4301.906	4271.281	3960.623	14.261	0.430	0.000

Ffar1	free fatty acid receptor 1	14.051	4.831	2.060	6.981	89.928	3.757	1.885	10.003	5.215	81.513	ND	ND
Figf	c-fos induced growth factor	17.564	14.494	12.362	14.807	17.661	7.513	6.598	22.007	12.039	71.799	ND	ND
Foxa2	forkhead box A2	66.743	183.586	117.441	122.590	47.795	184.076	210.194	106.032	166.767	32.498	1.360	0.196
Foxc2	forkhead box C2	10.538	7.247	4.121	7.302	43.949	1.878	3.770	8.002	4.550	68.911	ND	ND
Foxg1	forkhead box G1	10.538	7.247	4.121	7.302	43.949	2.817	1.885	8.002	4.235	77.822	ND	ND
Foxo1	forkhead box O1	105.383	132.858	123.622	120.621	11.591	46.019	61.267	56.017	54.434	14.230	0.451	0.001
Frap1	FK506 binding protein 12-rapamycin associated protein 1	186.177	135.274	156.588	159.346	16.043	87.342	115.937	142.043	115.107	23.769	0.722	0.055
G6pc	glucose-6-phosphatase, catalytic	5792.570	3379.431	3230.658	4134.220	34.785	1891.479	1479.841	2508.753	1960.024	26.422	0.474	0.035
G6pdx	glucose-6-phosphate dehydrogenase X-linked	45.666	57.975	70.053	57.898	21.060	27.236	30.162	20.006	25.801	20.262	ND	ND
Gata2	GATA binding protein 2	10.538	7.247	6.181	7.989	28.432	3.757	5.655	14.004	7.805	69.844	ND	ND
Gata3	GATA binding protein 3	10.538	7.247	6.181	7.989	28.432	2.817	2.828	8.002	4.549	65.738	ND	ND
Gcg	glucagon	14.051	7.247	20.604	13.967	47.818	8.452	22.622	24.007	18.360	46.886	ND	ND
Gcgr	glucagon receptor	1211.908	1500.091	1745.132	1485.710	17.965	760.724	885.077	832.250	826.017	7.556	0.556	0.007
Gck	glucokinase	133.486	229.482	117.441	160.136	37.836	339.039	368.546	500.150	402.578	21.307	2.514	0.008
Ghrl	ghrelin	14.051	2.416	6.181	7.549	78.646	3.757	3.770	8.002	5.176	47.279	ND	ND
Gip	gastric inhibitory polypeptide	10.538	7.247	4.121	7.302	43.949	3.757	2.828	10.003	5.529	70.576	ND	ND
Gja6	gap junction membrane channel protein alpha 6	1053.833	657.045	655.197	788.692	29.114	232.913	212.079	496.149	313.714	50.472	0.398	0.476
Gyk	glycerol kinase	14.051	7.247	4.121	8.473	59.926	5.635	2.828	16.005	8.156	85.102	ND	ND
Glp1r	glucagon-like peptide 1 receptor	10.538	7.247	8.241	8.676	19.459	7.513	4.713	12.004	8.077	45.537	ND	ND
Glp2r	glucagon-like peptide 2 receptor	14.051	7.247	10.302	10.533	32.355	3.757	4.713	14.004	7.491	75.563	ND	ND
Gpd1	glycerol-3-phosphate dehydrogenase 1 (soluble)	604.198	835.799	556.300	665.432	22.463	328.708	385.513	332.100	348.773	9.136	0.524	0.011
Grb2	growth factor receptor bound protein 2	344.252	442.056	541.877	442.728	22.319	293.959	365.719	262.079	307.252	17.277	0.694	0.052

Grb7	growth factor receptor bound protein 7	537.455	850.293	830.329	739.359	23.688	338.100	351.580	316.095	335.258	5.343	0.453	0.008
Gsk3a	glycogen synthase kinase 3 alpha	228.331	343.016	309.055	293.467	20.074	223.521	271.461	148.044	214.342	29.028	0.730	0.092
Gsk3b	glycogen synthase kinase 3 beta	277.509	202.911	206.037	228.819	18.441	136.179	149.869	196.059	160.702	19.524	0.702	0.044
Gys2	glycogen synthase 2	1078.423	543.511	581.024	734.319	40.662	403.841	310.107	550.165	421.371	28.712	0.574	0.084
Hbegf	heparin-binding EGF-like growth factor	14.051	9.662	10.302	11.338	20.910	8.452	9.426	12.004	9.961	18.422	ND	ND
Hk2	hexokinase 2	7.026	7.247	8.241	7.505	8.630	4.696	5.655	10.003	6.785	41.683	ND	ND
Hmgcs2	3-hydroxy-3-methylglutaryl-Coenzyme A synthase 2	10229.209	9865.330	8836.922	9643.820	7.488	3648.658	4235.926	4131.239	4005.275	7.821	0.415	0.000
Hmox1	heme oxygenase (decycling) 1	154.562	468.627	510.971	378.054	51.502	233.852	220.562	158.047	204.154	19.827	0.540	0.102
Hnf1a	HNF1 homeobox A	56.180	94.486	71.339	74.002	26.069	46.252	75.291	54.830	58.791	25.376	ND	ND
Hnf1b	HNF1 homeobox B	52.434	105.224	55.914	71.191	41.472	37.579	52.376	28.607	39.521	30.371	ND	ND
Hnf4a	hepatic nuclear factor 4, alpha	980.065	1388.973	1209.436	1192.825	17.183	630.180	884.134	610.183	708.166	21.566	0.594	0.015
Hp	haptoglobin	15940.985	65071.562	51783.249	44265.266	57.412	22268.554	41634.423	33193.958	32365.645	29.999	0.731	0.245
Hras1	Harvey rat sarcoma virus oncogene 1	259.946	318.860	247.244	275.350	13.878	278.932	369.489	364.109	337.510	15.052	1.226	0.083
Hsd11b1	hydroxysteroid 11-beta dehydrogenase 1	9969.263	4775.651	5637.169	6794.028	40.968	1922.472	2960.624	6479.944	3787.680	63.064	0.558	0.114
Hsd11b2	hydroxysteroid 11-beta dehydrogenase 2	10.538	2.416	2.060	5.005	95.819	1.878	0.943	8.002	3.608	106.285	ND	ND
Hsd17b10	hydroxysteroid (17-beta) dehydrogenase 10	2181.435	1630.533	1712.166	1841.378	16.146	748.515	972.736	1142.343	954.531	20.695	0.518	0.006
Iapp	islet amyloid polypeptide	14.051	2.416	4.121	6.862	91.565	2.817	1.885	8.002	4.235	77.822	ND	ND
Icam1	intercellular adhesion molecule	49.179	125.611	142.165	105.652	46.949	126.787	171.548	110.033	136.123	23.363	1.288	0.211
Ide	insulin degrading enzyme	941.424	611.148	729.371	760.648	22.000	494.940	470.344	1594.478	853.254	75.246	1.122	0.410
Igfbp1	insulin-like growth factor binding protein 1	2543.251	946.917	3259.503	2249.891	52.619	157.780	213.964	302.091	224.612	32.386	0.100	0.021
Igfbp2	insulin-like growth factor binding protein 2	4471.766	1173.984	1271.248	2305.666	81.388	465.826	744.633	862.259	690.906	29.469	0.300	0.106
Igfbp5	insulin-like growth factor binding protein 5	24.589	38.650	41.207	34.815	25.701	8.452	8.483	16.005	10.980	39.631	ND	ND

Ikbkb	inhibitor of kappaB kinase beta	101.871	214.989	150.407	155.755	36.434	223.521	226.218	186.056	211.932	10.593	1.361	0.093
Il10	interleukin 10	10.538	7.247	6.181	7.989	28.432	3.757	2.828	10.003	5.529	70.576	ND	ND
Il12b	interleukin 12b	10.538	2.416	4.121	5.692	75.254	3.757	1.885	8.002	4.548	68.919	ND	ND
Il23a	interleukin 23, alpha subunit p19	10.538	7.247	4.121	7.302	43.949	2.817	0.943	8.002	3.921	93.270	ND	ND
Il4ra	interleukin 4 receptor, alpha	87.819	115.949	140.105	114.625	22.829	60.107	65.980	72.022	66.036	9.022	0.576	0.017
Il6	interleukin 6	10.538	7.247	6.181	7.989	28.432	2.817	2.828	10.003	5.216	79.478	ND	ND
Inppl1	inositol polyphosphate phosphatase-like 1	21.077	157.014	86.535	88.209	77.072	84.525	99.913	38.011	74.150	43.464	ND	ND
Ins2	insulin II	10.538	4.831	2.060	5.810	74.405	1.878	1.885	10.003	4.589	102.179	ND	ND
Insig1	insulin induced gene 1	709.581	1345.492	1073.452	1042.842	30.595	1046.230	1184.815	770.231	1000.426	21.096	0.959	0.429
Insig2	insulin induced gene 2	3417.933	1787.548	2186.051	2463.844	34.497	2616.515	3184.957	8058.418	4619.963	64.748	1.875	0.148
Insl3	insulin-like 3	35.128	55.559	82.415	57.700	41.102	31.932	32.048	32.010	31.996	0.185	ND	ND
Insr	insulin receptor	63.230	36.234	37.087	45.517	33.715	12.209	14.139	20.006	15.451	26.281	ND	ND
Irs1	insulin receptor substrate 1	31.615	53.143	30.906	38.555	32.782	28.175	31.105	30.009	29.763	4.974	ND	ND
Irs2	insulin receptor substrate 2	165.101	171.508	168.950	168.520	1.914	38.506	41.473	48.014	42.664	11.403	0.253	0.000
Irs3	insulin receptor substrate 3	14.051	4.831	6.181	8.354	59.601	3.757	2.828	10.003	5.529	70.576	ND	ND
Jak2	Janus kinase 2	108.896	108.702	123.622	113.740	7.525	50.715	29.220	130.039	69.991	75.869	0.615	0.116
Jun	Jun oncogene	37.453	92.339	136.894	88.895	56.032	191.752	294.615	169.259	218.542	30.582	2.458	0.027
Katna1	katanin p60 (ATPase-containing) subunit A1	205.993	115.961	129.182	150.378	32.328	132.974	187.681	495.858	272.171	71.882	1.810	0.177
Kdr	kinase insert domain protein receptor	288.390	199.710	293.069	260.389	20.201	157.063	188.772	200.250	182.028	12.289	0.699	0.038
Khdrbs1	KH domain containing, RNA binding, signal transduction associated 1	116.105	191.120	185.096	164.107	25.398	151.282	145.125	159.723	152.043	4.820	0.926	0.324
Klf15	Kruppel-like factor 15	490.637	1078.005	630.483	733.042	41.856	261.129	493.207	276.536	343.624	37.766	0.469	0.056
Klf2	Kruppel-like factor 2 (lung)	71.161	94.486	67.483	77.710	18.845	46.252	55.650	64.366	55.422	16.346	ND	ND

Kras	v-Ki-ras2 Kirsten rat sarcoma viral oncogene homolog	456.929	328.555	416.466	400.650	16.381	256.311	223.689	572.144	350.715	54.875	0.875	0.346
Ldlr	low density lipoprotein receptor	191.011	575.509	283.428	349.983	57.347	507.805	727.808	436.260	557.291	27.265	1.592	0.113
Lef1	lymphoid enhancer binding factor 1	14.981	17.179	11.568	14.576	19.396	8.672	9.821	14.304	10.932	27.220	ND	ND
Lep	leptin	11.236	6.442	5.784	7.821	38.050	1.927	3.274	7.152	4.117	65.881	ND	ND
Lepr	leptin receptor	33.708	15.032	13.497	20.745	54.238	37.579	20.732	92.973	50.428	74.949	ND	ND
Lgals12	lectin, galactose binding, soluble 12	11.236	10.737	7.712	9.895	19.270	4.818	4.365	7.152	5.445	27.468	ND	ND
Lipc	lipase, hepatic	2588.015	1408.708	1581.028	1859.250	34.260	676.431	700.529	1094.225	823.728	28.476	0.443	0.029
Lipe	lipase, hormone sensitive	48.689	107.371	59.771	71.944	43.336	30.834	34.917	28.607	31.453	10.175	ND	ND
Lox	lysyl oxidase	7.491	15.032	5.784	9.436	52.154	2.891	4.365	11.920	6.392	75.782	ND	ND
Lpl	lipoprotein lipase	262.172	240.511	212.089	238.257	10.542	135.864	153.855	250.313	180.011	34.189	0.756	0.102
Map2k1	mitogen activated protein kinase kinase 1	404.494	339.292	375.976	373.254	8.757	447.100	557.586	786.698	597.128	29.008	1.600	0.046
Map2k6	mitogen activated protein kinase kinase 6	56.180	32.211	23.137	37.176	45.921	10.599	13.094	19.071	14.255	30.542	ND	ND
Mapk1	mitogen activated protein kinase 1	741.573	455.253	518.654	571.827	26.299	292.927	336.079	829.608	486.205	61.328	0.850	0.340
Mapk14	mitogen activated protein kinase 14	340.824	324.260	366.336	343.807	6.165	123.338	169.131	171.643	154.704	17.577	0.450	0.000
Mapk3	mitogen activated protein kinase 3	149.813	311.376	235.226	232.138	34.818	224.513	259.698	140.652	208.288	29.363	0.897	0.352
Mapk8	mitogen activated protein kinase 8	14.981	12.885	9.640	12.502	21.524	11.563	14.185	11.920	12.556	11.327	ND	ND
Mdh1	malate dehydrogenase 1, NAD (soluble)	9876.404	5997.745	6875.542	7583.231	26.821	3379.264	4072.235	7008.761	4820.087	39.976	0.636	0.081
Me1	malic enzyme 1, NADP(+)-dependent, cytosolic	337.079	392.978	321.990	350.682	10.664	211.023	322.985	319.447	284.485	22.372	0.811	0.098
Me2	malic enzyme 2, NAD(+)-dependent, mitochondrial	2606.742	1451.656	1492.336	1850.245	35.426	1969.551	1177.369	2460.218	1869.046	34.633	1.010	0.487
Me3	malic enzyme 3, NADP(+)-dependent, mitochondrial	29.963	47.243	52.058	43.088	26.966	30.834	44.738	42.911	39.494	19.130	ND	ND
Mif	macrophage migration inhibitory factor	7.491	15.032	7.712	10.078	42.581	10.599	10.912	9.536	10.349	6.970	ND	ND
Mlycd	malonyl-CoA decarboxylase	2359.551	1720.084	1675.504	1918.379	19.950	1979.187	2216.160	2729.602	2308.316	16.618	1.203	0.140

Mttp	microsomal triglyceride transfer protein	2662.921	1601.976	1760.339	2008.412	28.496	2261.515	2888.319	4646.284	3265.373	37.861	1.626	0.093
Nampt	nicotinamide phosphoribosyltransferase	453.184	208.300	321.990	327.824	37.382	207.169	193.137	660.349	353.552	75.176	1.078	0.443
Ncoa2	nuclear receptor coactivator 2	48.689	83.749	73.267	68.569	26.246	43.361	42.556	30.991	38.969	17.760	ND	ND
Neurod1	neurogenic differentiation 1	11.236	8.590	7.712	9.179	19.983	2.891	3.274	11.920	6.028	84.704	ND	ND
Nfkb1	nuclear factor of kappa light chain gene enhancer in B-cells 1, p105	86.142	204.005	169.671	153.273	39.549	111.775	142.943	83.438	112.718	26.405	0.735	0.179
Nfkbia	nuclear factor of kappa light chain gene enhancer in B-cells inhibitor, alpha	385.768	384.388	304.637	358.264	12.965	141.646	189.863	224.090	185.199	22.365	0.517	0.004
Nos2	nitric oxide synthase 2, inducible, macrophage	11.236	10.737	7.712	9.895	19.270	4.818	3.274	7.152	5.081	38.427	ND	ND
Nos3	nitric oxide synthase 3, endothelial cell	14.981	17.179	17.353	16.504	8.010	12.526	13.094	19.071	14.897	24.340	ND	ND
Npy	neuropeptide Y	7.491	8.590	5.784	7.288	19.396	1.927	4.365	4.768	3.687	41.691	ND	ND
Nr3c1	nuclear receptor subfamily 3, group C, member 1	408.240	246.953	281.500	312.231	27.198	143.573	94.932	438.644	225.716	82.403	0.723	0.252
Nr3c2	nuclear receptor subfamily 3, group C, member 2	41.199	27.916	34.705	34.607	19.192	14.454	18.550	16.688	16.564	12.382	ND	ND
Nr5a2	nuclear receptor subfamily 5, group A, member 2	535.581	367.209	381.760	428.183	21.788	186.934	223.689	348.054	252.892	33.388	0.591	0.037
Nsf	N-ethylmaleimide sensitive fusion protein	93.633	126.698	142.678	121.003	20.672	87.685	110.208	64.366	87.420	26.221	0.722	0.081
Pck2	phosphoenolpyruvate carboxykinase 2 (mitochondrial)	11.236	30.064	17.353	19.551	49.126	27.944	28.370	30.991	29.102	5.670	ND	ND
Pcx	pyruvate carboxylase	1779.026	2409.406	2086.185	2091.539	15.071	852.765	1477.440	989.332	1106.512	29.680	0.529	0.010
Pdha1	pyruvate dehydrogenase E1 alpha 1	891.386	579.804	622.771	697.987	24.193	590.673	653.609	1091.841	778.708	35.058	1.116	0.343
Pdhb	pyruvate dehydrogenase (lipoamide) beta	1516.854	989.961	1050.805	1185.873	24.307	1691.077	1259.207	3201.621	2050.635	49.736	1.729	0.115
Pdk4	pyruvate dehydrogenase kinase, isoenzyme 4	29.963	23.622	23.137	25.574	14.892	11.563	10.912	16.688	13.054	24.234	ND	ND
Pdpk1	3-phosphoinositide dependent protein kinase-1	164.794	139.582	138.822	147.733	10.005	95.394	109.117	183.563	129.358	36.675	0.876	0.278
Pdx1	pancreatic and duodenal homeobox 1	89.888	96.634	75.195	87.239	12.566	50.106	65.470	64.366	59.981	14.287	ND	ND
Pfkfb1	6-phosphofructo-2-kinase/fructose-2,6-biphosphatase 1	408.240	296.344	352.839	352.474	15.873	149.354	125.484	207.402	160.747	26.209	0.456	0.005
Pfkm	phosphofructokinase, muscle	48.689	88.044	55.914	64.216	32.624	48.179	63.288	59.598	57.022	13.814	ND	ND

Pi4k2b	phosphatidylinositol 4-kinase type 2 beta	239.700	171.794	175.456	195.650	19.521	147.427	193.137	402.885	247.816	54.970	1.267	0.279
Pi4ka	phosphatidylinositol 4-kinase, catalytic, alpha polypeptide	153.558	158.909	154.247	155.571	1.871	78.050	108.026	85.822	90.632	17.164	0.583	0.001
Pik3c3	phosphoinositide-3-kinase, class 3	179.775	120.256	140.750	146.927	20.579	66.487	76.382	71.518	71.462	6.923	0.486	0.006
Pik3cb	phosphatidylinositol 3-kinase, catalytic, beta polypeptide	82.397	81.602	98.332	87.444	10.793	261.129	285.886	424.340	323.785	27.166	3.703	0.005
Pik3cg	phosphoinositide-3-kinase, catalytic, gamma polypeptide	11.236	10.737	7.712	9.895	19.270	4.818	4.365	11.920	7.034	60.237	ND	ND
Pik3r1	phosphatidylinositol 3-kinase, regulatory subunit, polypeptide 1 (p85 alpha)	101.124	118.108	100.260	106.497	9.450	50.106	48.011	59.598	52.572	11.745	0.494	0.001
Pip	prolactin induced protein	14.981	15.032	9.640	13.218	23.440	3.854	6.547	14.304	8.235	65.881	ND	ND
Pklr	pyruvate kinase liver and red blood cell	1000.000	712.944	651.692	788.212	23.592	1871.266	818.375	1194.350	1294.664	41.213	1.643	0.098
Pkm2	pyruvate kinase, muscle	59.925	206.152	121.469	129.182	56.833	90.576	160.402	114.429	121.802	29.139	0.943	0.442
Plcg1	phospholipase C, gamma 1	138.577	191.120	188.952	172.883	17.197	79.013	91.658	61.982	77.551	19.203	0.449	0.004
Plin	perilipin	11.236	6.442	5.784	7.821	38.050	2.891	3.274	7.152	4.439	53.111	ND	ND
Pnpla2	patatin-like phospholipase domain containing 2	232.210	240.511	250.651	241.124	3.830	142.609	172.404	233.625	182.880	25.374	0.758	0.050
Ppara	peroxisome proliferator activated receptor alpha	479.401	560.477	541.791	527.223	8.053	149.354	161.493	159.723	156.857	4.180	0.298	0.000
Ppard	peroxisome proliferator activator receptor delta	89.888	264.133	183.168	179.063	48.695	106.957	122.211	50.063	93.077	40.852	0.520	0.096
Pparg	peroxisome proliferator activated receptor gamma	82.397	55.833	55.914	64.715	23.663	50.106	44.738	76.286	57.043	29.590	ND	ND
Ppargc1a	peroxisome proliferative activated receptor, gamma, coactivator 1 alpha	29.963	27.916	34.705	30.861	11.285	8.672	7.638	11.920	9.410	23.741	ND	ND
Ppargc1b	peroxisome proliferative activated receptor, gamma, coactivator 1 beta	22.472	47.243	17.353	29.023	55.080	10.599	10.912	11.920	11.144	6.192	ND	ND
Ppp1ca	protein phosphatase 1, catalytic subunit, alpha isoform	1142.322	1576.207	1667.791	1462.107	19.198	909.616	1073.708	958.341	980.555	8.594	0.671	0.023
Ppp1r10	protein phosphatase 1, regulatory subunit 10	63.670	73.012	79.051	71.911	10.776	42.397	92.749	45.295	60.147	47.004	ND	ND
Ppp1r1b	protein phosphatase 1, regulatory (inhibitor) subunit 1B	93.633	83.749	80.979	86.121	7.724	14.454	17.459	26.223	19.379	31.556	ND	ND
Ppp2r2b	protein phosphatase 2 (formerly 2A), regulatory subunit B (PR 52), beta isoform	14.981	10.737	7.712	11.144	32.768	4.818	4.365	11.920	7.034	60.237	ND	ND
Prkaa1	protein kinase, AMP-activated, alpha 1 catalytic subunit	119.850	85.897	82.908	96.218	21.327	45.288	41.464	104.893	63.882	55.678	ND	ND

Prkaa2	protein kinase, AMP-activated, alpha 2 catalytic subunit	408.240	186.826	242.938	279.335	41.207	184.043	110.208	359.974	218.075	58.839	0.781	0.286
Prkab1	protein kinase, AMP-activated, beta 1 non-catalytic subunit	86.142	118.108	138.822	114.357	23.207	74.195	92.749	52.447	73.130	27.584	0.639	0.049
Prkaca	protein kinase, cAMP dependent, catalytic, alpha	539.326	513.233	563.000	538.520	4.623	439.391	604.507	674.653	572.850	21.085	1.064	0.327
Prkag2	protein kinase, AMP-activated, gamma 2 non-catalytic subunit	213.483	150.319	179.312	181.038	17.464	177.298	201.866	328.983	236.049	34.491	1.304	0.168
Prkcb	protein kinase C, beta 1	18.727	30.064	28.921	25.904	24.097	13.490	12.003	16.688	14.060	17.025	ND	ND
Prkcq	protein kinase C, theta	11.236	17.179	19.281	15.899	26.244	6.745	7.638	9.536	7.973	17.875	ND	ND
Prl	prolactin	7.491	6.442	3.856	5.930	31.547	0.964	1.091	4.768	2.274	95.001	ND	ND
Pten	phosphatase and tensin homolog	2831.461	1868.256	1854.815	2184.844	25.632	886.491	843.472	2608.022	1445.995	69.611	0.662	0.164
Ptk2	PTK2 protein tyrosine kinase 2	33.708	53.686	53.986	47.127	24.661	40.470	39.282	45.295	41.682	7.640	ND	ND
Ptpn1	protein tyrosine phosphatase, non-receptor type 1	78.652	85.897	142.678	102.409	34.237	66.487	68.744	107.277	80.836	28.362	0.789	0.211
Ptprf	protein tyrosine phosphatase, receptor type, F	265.918	388.683	331.630	328.744	18.687	221.623	304.436	245.545	257.201	16.570	0.782	0.086
Pygb	brain glycogen phosphorylase	18.727	40.801	34.705	31.411	36.293	32.762	33.826	19.071	28.553	28.818	ND	ND
Pygl	liver glycogen phosphorylase	6737.828	4273.367	4646.679	5219.291	25.449	4881.480	5556.222	9771.738	6736.480	39.341	1.291	0.213
Pygm	muscle glycogen phosphorylase	18.727	17.179	13.497	16.468	16.315	10.599	12.003	16.688	13.097	24.343	ND	ND
Rab3il1	RAB3A interacting protein (rabin3)-like 1	18.727	47.243	26.993	30.988	47.348	18.308	27.279	16.688	20.758	27.484	ND	ND
Rab4a	RAB4A, member RAS oncogene family	235.955	212.595	268.003	238.851	11.646	175.371	214.960	188.331	192.887	10.464	0.808	0.041
Raf1	v-raf-leukemia viral oncogene 1	531.835	536.855	580.353	549.681	4.854	361.341	449.561	283.688	364.863	22.746	0.664	0.011
Rara	retinoic acid receptor, alpha	29.963	34.359	26.993	30.438	12.175	14.454	16.368	19.071	16.631	13.951	ND	ND
Rasgrp4	RAS guanyl releasing protein 4	7.491	8.590	5.784	7.288	19.396	2.891	4.365	7.152	4.802	45.061	ND	ND
Rbp4	retinol binding protein 4, plasma	26614.232	24648.091	21251.326	24171.216	11.224	12547.697	17099.678	17867.573	15838.316	18.155	0.655	0.011
Retn	resistin	7.491	6.442	3.856	5.930	31.547	1.927	2.182	4.768	2.959	53.111	ND	ND
Rgs2	regulator of G-protein signaling 2	119.850	135.287	152.319	135.819	11.958	70.341	73.108	152.572	98.674	47.325	0.727	0.132

Rhoj	ras homolog gene family, member J	37.453	62.275	57.842	52.524	25.204	27.944	33.826	30.991	30.920	9.514	ND	ND
Rhoq	ras homolog gene family, member Q	29.963	70.865	57.842	52.890	39.509	37.579	34.917	26.223	32.907	18.048	ND	ND
Rorc	RAR-related orphan receptor gamma	378.277	373.651	358.623	370.184	2.776	277.510	326.259	278.920	294.230	9.430	0.795	0.006
Rps6ka1	ribosomal protein S6 kinase polypeptide 1	29.963	49.391	32.777	37.377	28.090	25.053	22.915	23.839	23.936	4.481	ND	ND
Rxra	retinoid X receptor alpha	419.476	485.317	460.812	455.201	7.310	237.040	380.817	233.625	283.828	29.600	0.624	0.015
Rxrb	retinoid X receptor beta	41.199	96.634	67.483	68.438	40.518	56.851	78.564	42.911	59.442	30.227	ND	ND
Scara3	scavenger receptor class A, member 3	7.491	8.590	7.712	7.931	7.328	1.927	2.182	7.152	3.754	78.469	ND	ND
Sell	selectin, lymphocyte	22.472	30.064	25.065	25.867	14.919	14.454	17.459	21.455	17.789	19.745	ND	ND
Serpina12	serine (or cysteine) peptidase inhibitor, clade A (alpha-1 antiproteinase, antitrypsin), member 12	86.142	51.538	40.490	59.390	40.104	67.450	27.279	47.679	47.469	42.314	ND	ND
Serpine1	serine (or cysteine) peptidase inhibitor, clade E, member 1	11.236	10.737	5.784	9.252	32.574	4.818	7.638	7.152	6.536	23.067	ND	ND
Sfrp2	secreted frizzled-related protein 2	11.236	19.327	7.712	12.758	46.675	3.854	5.456	7.152	5.487	30.051	ND	ND
Slc17a3	solute carrier family 17 (sodium phosphate), member 3	782.772	502.496	589.993	625.087	22.940	237.040	270.609	772.394	426.681	70.279	0.683	0.180
Slc27a1	solute carrier family 27 (fatty acid transporter), member 1	18.727	49.391	21.209	29.775	57.204	9.636	16.368	9.536	11.846	33.055	ND	ND
Slc2a1	solute carrier family 2 (facilitated glucose transporter), member 1	41.199	137.435	115.685	98.106	51.443	123.338	187.681	102.509	137.843	32.211	1.405	0.182
Slc2a2	solute carrier family 2 (facilitated glucose transporter), member 2	2445.693	1028.614	1118.288	1530.865	51.836	518.404	373.179	1230.109	707.231	64.846	0.462	0.097
Slc2a3	solute carrier family 2 (facilitated glucose transporter), member 3	7.491	8.590	5.784	7.288	19.396	1.927	3.274	4.768	3.323	42.765	ND	ND
Slc2a4	solute carrier family 2 (facilitated glucose transporter), member 4	29.963	21.474	19.281	23.573	23.933	14.454	14.185	21.455	16.698	24.686	ND	ND
Slc2a5	solute carrier family 2 (facilitated glucose transporter), member 5	14.981	19.327	11.568	15.292	25.428	4.818	4.365	7.152	5.445	27.468	ND	ND
Slc6a6	solute carrier family 6 (neurotransmitter transporter, taurine), member 6	374.532	326.408	356.695	352.545	6.901	183.080	241.148	269.384	231.204	19.032	0.656	0.007
Smarcd2	SWI/SNF related, matrix associated, actin dependent regulator of chromatin, subfamily d, member 2	119.850	201.858	165.815	162.508	25.293	79.013	111.299	78.670	89.661	20.901	0.552	0.025

Snap23	synaptosomal-associated protein 23	247.191	231.921	250.651	243.254	4.097	139.719	127.667	288.456	185.280	48.335	0.762	0.164
Snap25	synaptosomal-associated protein 25	7.491	6.442	5.784	6.572	13.094	1.927	2.182	4.768	2.959	53.111	ND	ND
Socs3	suppressor of cytokine signaling 3	14.981	70.865	291.140	125.662	116.190	15.417	29.462	11.920	18.933	49.038	0.151	0.138
Sparc	secreted acidic cysteine rich glycoprotein	464.419	1110.216	657.476	744.037	44.552	450.954	628.512	688.956	589.474	20.987	0.792	0.246
Spock3	sparc/osteonectin, cwcv and kazal-like domains proteoglycan 3	7.491	8.590	5.784	7.288	19.396	2.891	3.274	7.152	4.439	53.111	ND	ND
Srebf1	sterol regulatory element binding factor 1	397.004	1026.467	759.665	727.712	43.416	421.083	389.547	188.331	332.987	37.919	0.458	0.057
Stat3	signal transducer and activator of transcription 3	475.655	940.570	1172.274	862.833	41.115	384.467	572.863	274.152	410.494	36.796	0.476	0.056
Stk11	serine/threonine kinase 11	389.513	448.811	383.688	407.337	8.846	233.186	258.607	267.000	252.931	6.961	0.621	0.001
Stx4a	syntaxin 4A (placental)	198.502	343.587	273.788	271.959	26.680	165.735	187.681	169.259	174.225	6.764	0.641	0.041
Stxbp1	syntaxin binding protein 1	14.981	17.179	13.497	15.219	12.175	9.636	10.912	7.152	9.233	20.708	ND	ND
Stxbp2	syntaxin binding protein 2	161.049	219.037	206.305	195.463	15.592	143.573	177.860	185.947	169.127	13.302	0.865	0.147
Syp	synaptophysin	11.236	8.590	5.784	8.537	31.936	1.927	3.274	9.536	4.912	82.660	ND	ND
Tcf7	transcription factor 7, T-cell specific	18.727	30.064	19.281	22.690	28.169	8.672	9.821	9.536	9.343	6.400	ND	ND
Tcf3	transcription factor 3	26.217	27.916	23.137	25.757	9.406	8.672	10.912	14.304	11.296	25.100	ND	ND
Tcf7l2	transcription factor 7-like 2, T-cell specific, HMG-box	78.652	107.371	82.908	89.643	17.290	30.834	45.829	28.607	35.090	26.693	ND	ND
Tek	endothelial-specific receptor tyrosine kinase	86.142	120.256	107.973	104.790	16.488	54.924	51.285	64.366	56.858	11.875	0.543	0.006
Trf	transferrin	94078.652	110847.694	118465.246	107797.197	11.574	43065.138	50832.015	43463.854	45787.002	9.552	0.425	0.001
Tcfap2a	transcription factor AP-2, alpha	3.745	6.442	1.928	4.039	56.241	2.891	1.091	2.384	2.122	43.731	ND	ND
Tg	thyroglobulin	7.491	6.442	5.784	6.572	13.094	2.891	3.274	4.768	3.644	27.220	ND	ND
Tgfb1	transforming growth factor, beta 1	48.689	120.256	77.123	82.023	43.932	64.560	84.020	54.830	67.803	21.920	ND	ND
Thbs1	thrombospondin 1	11.236	25.769	7.712	14.906	64.213	6.745	6.547	9.536	7.609	21.964	ND	ND
Thbs2	thrombospondin 2	7.491	12.885	7.712	9.362	32.600	4.818	4.365	7.152	5.445	27.468	ND	ND

Thbs4	thrombospondin 4	11.236	6.442	3.856	7.178	52.166	2.891	4.365	7.152	4.802	45.061	ND	ND
Thrb	thyroid hormone receptor beta	86.142	75.160	98.332	86.545	13.394	38.543	39.282	45.295	41.040	9.023	ND	ND
Tnf	tumor necrosis factor	7.491	8.590	7.712	7.931	7.328	2.891	5.456	9.536	5.961	56.220	ND	ND
Tnfrsf1a	tumor necrosis factor receptor superfamily, member 1a	310.861	560.477	611.202	494.180	32.533	275.583	343.718	340.902	320.068	12.045	0.648	0.071
Tnfrsf1b	tumor necrosis factor receptor superfamily, member 1b	56.180	156.762	140.750	117.897	45.841	65.523	97.114	38.143	66.927	44.094	0.568	0.112
Tradd	TNFRSF1A-associated via death domain	63.670	88.044	65.555	72.423	18.725	50.106	54.558	50.063	51.576	5.009	ND	ND
Traf2	Tnf receptor-associated factor 2	52.434	100.929	75.195	76.186	31.846	71.305	91.658	61.982	74.982	20.239	ND	ND
Trib3	tribbles homolog 3 (Drosophila)	33.708	21.474	17.353	24.178	35.181	46.252	50.194	64.366	53.604	17.772	ND	ND
Tshb	thyroid stimulating hormone, beta subunit	7.491	6.442	3.856	5.930	31.547	2.891	2.182	4.768	3.280	40.730	ND	ND
Tshr	thyroid stimulating hormone receptor	11.236	8.590	5.784	8.537	31.936	2.891	2.182	7.152	4.075	65.965	ND	ND
Ucp1	uncoupling protein 1 (mitochondrial, proton carrier)	7.491	6.442	1.928	5.287	55.906	0.964	2.182	4.768	2.638	73.642	ND	ND
Ucp2	uncoupling protein 2 (mitochondrial, proton carrier)	119.850	427.337	294.997	280.728	54.943	165.735	200.775	140.652	169.054	17.863	0.602	0.143
Ucp3	uncoupling protein 3 (mitochondrial, proton carrier)	11.236	12.885	9.640	11.254	14.414	8.672	4.365	11.920	8.319	45.558	ND	ND
Vamp3	vesicle-associated membrane protein 3	71.161	107.371	156.175	111.569	38.238	83.831	105.843	102.509	97.394	12.181	0.873	0.304
Vapa	vesicle-associated membrane protein, associated protein A	1363.296	916.949	1045.021	1108.422	20.735	844.093	912.216	1663.985	1140.098	39.907	1.029	0.460
Vdr	vitamin D receptor	11.236	8.590	7.712	9.179	19.983	2.891	3.274	7.152	4.439	53.111	ND	ND
Vegfa	vascular endothelial growth factor A	179.775	433.779	362.480	325.345	40.268	233.186	282.612	157.340	224.379	28.122	0.690	0.148
Vegfb	vascular endothelial growth factor B	74.906	66.570	57.842	66.440	12.843	43.361	46.920	69.134	53.138	26.283	ND	ND
Vegfc	vascular endothelial growth factor C	37.453	47.243	42.418	42.371	11.553	30.834	32.735	61.982	41.851	41.721	ND	ND
Vldlr	very low density lipoprotein receptor	52.434	34.359	26.993	37.929	34.515	94.431	100.387	297.992	164.270	70.521	4.331	0.067
Wnt10b	wingless related MMTV integration site 10b	7.491	8.590	5.784	7.288	19.396	5.781	6.547	7.152	6.493	10.576	ND	ND

Mice were treated with TCPOBOP (3 mg/kg/day) or corn oil for 5 days (n=3). Hepatic RNA was subjected to DNA microarray analysis. ND, Not detected.

Table S2. Primers used for quantitative RT-PCR.

Gene	Forward primer (5' to 3')	Reverse primer (5' to 3')
mAcat1	GCGGGCTGCTGCAGGAAGTAA	GTGGCCGGCTGAGAGGCAAG
mAcox1	AGCTGCGGAGACAGGTTGTCA	TCAAGTTCTCGATTTCTCGACGGC
mCpt1a	TGCAGACTCGGTCACCACTCAAGAT	CTCGCGGGGAACACACCAGTG
mCyp4a10	TGTCCCAGGCATTGTCAGAGA	CCTTCGGGTTGTGGTGGAGA
mG0s2	CCAGTCTGACGCAAGGACGCC	TGGCTGGGCCTAGGGTGCAGT
mGyk	AACTCAGTCTCCAGAAAGTGGTATCCC	TAGAGGATCATGCAGCCAGTGGC
mHmgcs2	TCTGTGTCCCATTGTTGGGCCC	TCCCTGGGCCATCTTCCCAGTTC
mPdk4	CTACGGATCCTAACCACCGC	TCTGAACCAAAGTCCAGCAGC
mVnn1	ACTTTCCTCGCGGCTGTTTA	CAATAATGTGCGCACCCTGC
hACAT1	AGGCAGTATTGGGTGCAGGCTT	GCTCTCCATCCCACCTGCCAC
hACOX1	CGGGCGAGACCTCCCTCCTT	TCATGTTCTCTGGGGAATGGCGA
hCPT1A	GGGCTTTGGACCGGTTGCTGAT	CAGGTGCCTTCCAAAGCGATGAGA
hCYP4A11	GCCATTAGTGACCTGAACAACCTGG	ACTTGGTCTGTGTGCTGATGGGC
hHMGCS2	TGCTACGGTGGTACTGCCTCCC	CCACCATGGCATAACGACCATCCC
mACTB	GCCAACACAGTGCTGTCTG	CCTGCTTGCTGATCCACATC
human/green monkey GAPDH	CATGGGTGTGAACCATGAGAA	GGTCATGAGTCCTTCCACGAT
human/green monkey PGC1A	CAAGCCAAACCAACAACTTTATCTCT	CACACTTAAGGTGCGTTCAATAGTC